


RESEARCH ARTICLE

Open Access



Keratinocytes drive the epithelial hyperplasia key to sea lice resistance in coho salmon

S. J. Salisbury^{1*†} , R. Ruiz Daniels^{1†}, S. J. Monaghan², J. E. Bron², P. R. Villamayor^{1,3}, O. Gervais¹, M. D. Fast⁴, L. Sveen⁵, R. D. Houston⁶, N. Robinson^{5,7*} and D. Robledo^{1,3*}

Abstract

Background Salmonid species have followed markedly divergent evolutionary trajectories in their interactions with sea lice. While sea lice parasitism poses significant economic, environmental, and animal welfare challenges for Atlantic salmon (*Salmo salar*) aquaculture, coho salmon (*Oncorhynchus kisutch*) exhibit near-complete resistance to sea lice, achieved through a potent epithelial hyperplasia response leading to rapid louse detachment. The molecular mechanisms underlying these divergent responses to sea lice are unknown.

Results We characterized the cellular and molecular responses of Atlantic salmon and coho salmon to sea lice using single-nuclei RNA sequencing. Juvenile fish were exposed to copepodid sea lice (*Lepeophtheirus salmonis*), and lice-attached pelvic fin and skin samples were collected 12 h, 24 h, 36 h, 48 h, and 60 h after exposure, along with control samples. Comparative analysis of control and treatment samples revealed an immune and wound-healing response that was common to both species, but attenuated in Atlantic salmon, potentially reflecting greater sea louse immunomodulation. Our results revealed unique but complementary roles of three layers of keratinocytes in the epithelial hyperplasia response leading to rapid sea lice rejection in coho salmon. Our results suggest that basal keratinocytes direct the expansion and mobility of intermediate and, especially, superficial keratinocytes, which eventually encapsulate the parasite.

Conclusions Our results highlight the key role of keratinocytes in coho salmon's sea lice resistance and the diverged biological response of the two salmonid host species when interacting with this parasite. This study has identified key pathways and candidate genes that could be manipulated using various biotechnological solutions to improve Atlantic salmon sea lice resistance.

Keywords snRNAseq, Salmon, Aquaculture, Disease, Parasite, Sea lice, Cell type, Skin, Immunity, Wound healing

[†]S. J. Salisbury and R. Ruiz Daniels are co-first authors.

*Correspondence:

S. J. Salisbury
sarah.salisbury@roslin.ed.ac.uk
N. Robinson
nicholas.robinson@nofima.no
D. Robledo
diego.robledo@roslin.ed.ac.uk

Full list of author information is available at the end of the article



Background

Parasitism by sea lice is one of the greatest economic, environmental, and animal welfare issues facing the Atlantic salmon (*Salmo salar*, Linnaeus, 1758) aquaculture industry, with annual global costs exceeding £700 million [1]. Sea lice species, including the northern hemisphere's *Lepeophtheirus salmonis* (Krøyer, 1837) and the southern hemisphere's *Caligus rogercresseyi* (Boxshall and Bravo 2000) [2], feed on salmon skin and fins, causing chronic open wounds in Atlantic salmon that can contribute to secondary infections [3]. Additionally, sea lice significantly reduce the market value of aquaculture fish—infestations have been estimated to cost US\$0.46/kg of biomass [4]—and can also cause considerable impacts on wild salmonids [5]. A variety of treatment strategies have been developed to mitigate sea lice infestations in Atlantic salmon aquaculture, but these can be costly, ineffective, environmentally damaging, and cause reduced animal welfare [6]. For example, sea lice have evolved increasing resistance to the costly and potentially environmentally damaging chemical parasiticides that have historically been commonly applied to salmon aquaculture pens [5, 7]. Preventative methods, particularly those improving the innate resistance of Atlantic salmon to sea lice, are therefore considered a more effective route to address this problem [6].

Relatively high heritabilities for sea lice resistance in Atlantic salmon (e.g. [8–10]) suggest that selective breeding should be effective, particularly when informed by genotype information via genomic selection [11, 12]. However, counts of sessile lice are the only measure of resistance that is currently used, doubts have been raised about the efficacy of selection for reduced count for sea lice control in the sea cage environment [13], and genetic variation in the immune response of Atlantic salmon has been difficult to assess. In addition, despite the identification of some significant QTL (e.g. [14–16]), sea lice resistance has proven to be a polygenic trait [11]. Given the absence of loci of large effect to target, the relatively long generation time of Atlantic salmon (3–4 years), and the fact that modern salmon breeding programs must include multiple additional traits in their breeding goal, selective breeding is unlikely to result in clear improvements to sea lice resistance in the short term [6]. More rapid increases in genetic resistance to sea lice through gene editing or other biotechnological approaches may be informed by investigation of closely related salmonid species demonstrating greater resistance to sea lice [17].

Coho salmon (*Oncorhynchus kisutch*, Walbaum, 1792) demonstrate an innate ability to kill and expel sea lice. Within 24 h of louse attachment, coho salmon mount an acute epithelial hyperplasia response associated with a thickening of the skin, inflammation, cell proliferation,

and an infiltration of immune cells [18–20]. This localized swelling can even encapsulate attached lice after 10 days post exposure [18, 20] and causes 90% of lice to drop off their coho salmon hosts between 7 and 14 days post exposure [19, 21]. In contrast, minimal swelling and rapid degradation of the epidermis occurs in response to an attached louse in highly susceptible Atlantic salmon [18]. The resistance of coho salmon to sea lice has therefore been proposed to be the result of an immune and wound-healing response that is greater in magnitude and very different in character to that of Atlantic salmon [22, 23]. This is supported by the upregulation of multiple genes associated with inflammation, tissue remodelling, and cell adhesion in the skin of coho salmon but not Atlantic salmon in response to sea lice [23, 24]. Both Atlantic salmon and coho salmon have also been suggested to mount a nutritional immune response to sea lice [25, 26], where iron availability is limited to deter iron-seeking pathogens [27]. However, the exact molecular and cellular mechanisms underlying coho salmon's resistance to sea lice remain elusive.

This uncertainty is in part due to the cellular heterogeneity of fish skin. The skin's multiple layers demonstrate distinct transcriptomic profiles reflecting each layer's unique composition of cell types [28]. The outermost layer of skin, the epidermis, is populated primarily by filament-filled keratinocytes [29] in three layers: an upper layer of flattened superficial keratinocytes, an intermediate layer of amorphous keratinocytes, and a lower layer of cuboidal basal keratinocytes [30, 31]. Specialized mucous cells are found individually throughout the epithelium and play an important role in maintaining skin integrity through mucus production [31, 32]. The dermal layer below contains fibroblasts, blood vessels, and chromatophores [31, 32] as well as scales in the trunk and fin rays in the fins, both maintained by osteoblasts [31, 33, 34]. Both epidermal and dermal layers are punctuated by endothelial blood vessels and neural structures [35]. Muscle and fat lie below the dermis and are not considered part of the skin [31]. There is also a variety of resident immune cells in the skin including T cells, B cells, neutrophils, dendritic cells, and macrophages [36].

The large diversity of specialized cell types present within the skin therefore poses a problem for traditional bulk transcriptomic approaches which average gene expression across all cell types within a tissue and may therefore be unable to detect biologically relevant cell-type specific differential gene expression in highly heterogeneous tissues [37]. Single-nuclei RNA sequencing (snRNAseq) offers a solution to this issue by generating individual transcriptomes for thousands of individual cells [38]. Cells can be grouped based on their individual transcriptomes into distinct cell type clusters, whose

identities can be ascertained from diagnostic marker genes, uniquely expressed in each cluster. These technologies allow the study of biological processes with unparalleled resolution, facilitating the comparison of the same cell type across groups or species.

The aim of this work was therefore to use snRNAseq to investigate the cell types and gene expression patterns characterizing the response to sea lice in the skin of Atlantic salmon and coho salmon. We specifically targeted the first 60 h post infection by *L. salmonis* copepodids. This time frame has been largely unexplored from a transcriptomic perspective despite being associated with significant histological changes leading to sea lice rejection in coho salmon [24]. Comparing the cell type-specific responses of resistant and susceptible species to sea lice allowed us to identify cell types and molecular pathways involved in determining the mechanisms of resistance in coho salmon and to pinpoint candidate genes that could be targeted to improve sea lice resistance in Atlantic salmon aquaculture.

Results

A total of 10 and 12 snRNAseq libraries passed filtration for Atlantic salmon and coho salmon, respectively. These had over 244 million reads each, and of those reads

aligning to the genome, at least 73% and 86% aligned uniquely, for Atlantic salmon and coho salmon, respectively (Additional file 1: Tables S1, S2). The final total number of cells obtained for each species was 50,328 for Atlantic and 48,341 for coho salmon (Additional file 1: Table S3).

Cell type identities and marker genes

A total of 23 cell clusters were observed within each species, after clustering cells independently by species (Fig. 1a, b). These clusters demonstrated distinct transcriptomic profiles and their inferred identities were consistent across species (Fig. 1). Marker genes were frequently identical for the same cell type across species (Fig. 1c, d, see Additional file 1: Figs. S1, S2 for dot plots of additional cell markers, Table 1 for functional relevance of all marker genes for ascribed cell type identity, Additional file 1: Tables S4, S5 for counts per cell type and sample, Additional file 2 for all detected marker genes) and highly concordant between fin and skin tissue types (Additional file 1: Figs. S3, S4). We identified all cell types expected in these tissues [31, 93] as well as several previously unreported cell types including a tuft-like “secretory” cell type.

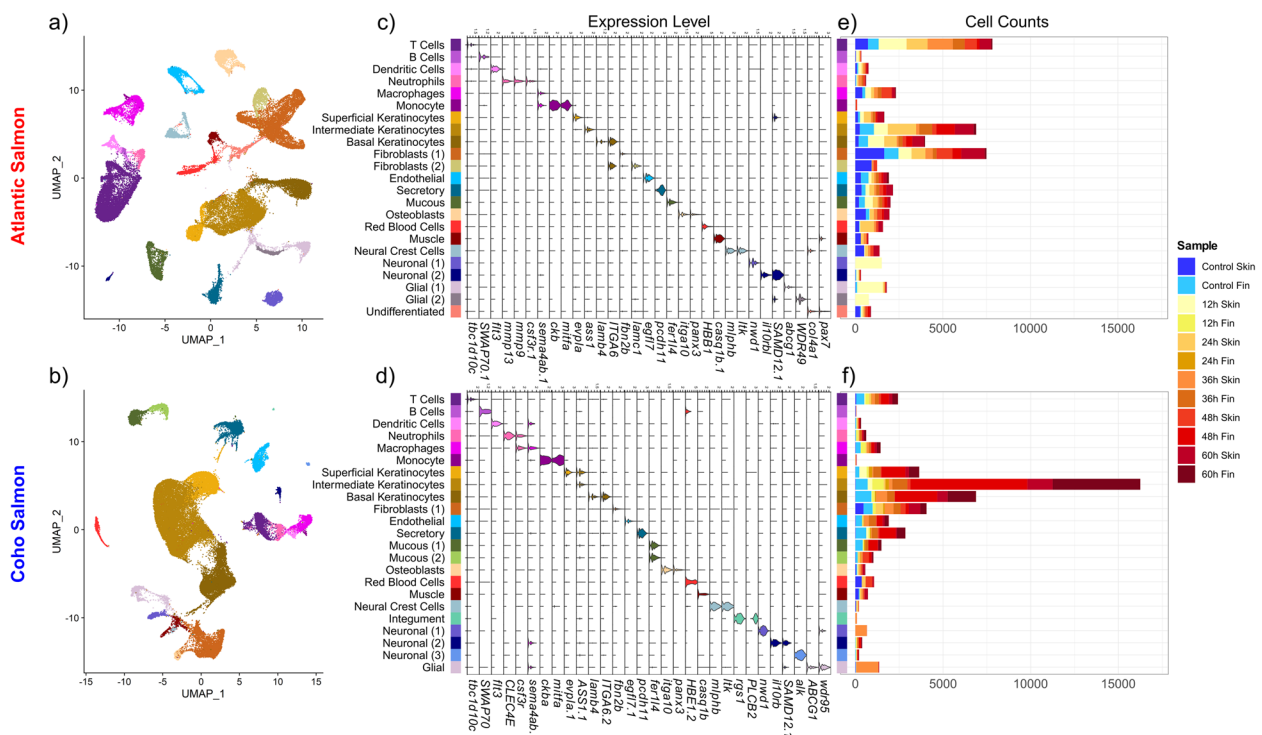


Fig. 1 Cell types detected in Atlantic (a–c) and coho (d–f) salmon. UMAPs of cell clusters coloured by putative identity for a Atlantic salmon and b coho salmon. Violin plots of marker genes for each cell cluster for c Atlantic salmon and d coho salmon. Counts of each cell type by sample for e Atlantic salmon and f coho salmon. Note there is no 12 h fin or 24 h fin sample for Atlantic salmon

Table 1 Marker genes for cell types found in skin and fin samples of Atlantic salmon and coho salmon. All noted genes were significantly ($p_{adj} < 0.001$) upregulated in the given species' cell type cluster relative to all other cells. See footnote for reference hyperlinks [28, 39–92]

	Cell Type	Marker Gene	Atlantic Salmon ENSEMBL ID	Coho Salmon ENSEMBL ID	Support for Cell Type Identity	
Both Species	T Cells	<i>tbc1d10c</i>	ENSSSAG0000005420	ENSOKIG00005011012	Expressed in T cells [39]	
		<i>tbc11b</i>	ENSSSAG00000071984	ENSOKIG00005023187	Expressed in T cells [40]	
			ENSSSAG00000045088			
		<i>tcf7</i>	ENSSSAG00000006857	ENSOKIG00005033777	Expressed in T cells [40]	
		<i>skap1</i>	ENSSSAG00000066533	ENSOKIG00005050132	Expressed in T cells [41]	
		<i>cd3</i>	ENSSSAG00000076824		Marker for T cells [42]	
		<i>cd2</i>		ENSOKIG00005012541	Marker for T cells [43]	
	B Cells	<i>chf1</i>	ENSSSAG00000079780	ENSOKIG00005001939	Marker for B cells [44]	
			ENSSSAG00000070298			
		<i>swap70</i>	ENSSSAG00000115076	ENSOKIG00005020004	Marker for B cells [45]	
	Dendritic Cells	<i>cd79</i>	ENSSSAG00000113980	ENSOKIG00005014962	Marker for B cells [46]	
		<i>flt3</i>	ENSSSAG00000009390	ENSOKIG00005021723	Marker for dendritic cells [47]	
	Neutrophils		ENSSSAG00000060395			
		<i>blnk</i>	ENSSSAG00000023874		Expressed in dendritic cells [48]	
		<i>csf3r</i>	ENSSSAG00000072535	ENSOKIG00005018820	Expressed in neutrophils [49]	
	Macrophages	<i>mmp9</i>	ENSSSAG00000069874		Marker for neutrophils in Atlantic Salmon [50]	
		<i>mmp13</i>	ENSSSAG00000070495		Marker for neutrophils in Atlantic Salmon [50]	
		<i>clec4e</i>		ENSOKIG00005020977	Expressed in neutrophils [51]	
		<i>sema4ab</i>	ENSSSAG00000056722	ENSOKIG00005023500	Expressed in macrophages [52]	
		<i>csf1r</i>	ENSSSAG00000047020		Expressed in macrophages [53]	
Monocyte		ENSSSAG00000061479				
	<i>marco</i>	ENSSSAG00000063051		Marker gene for macrophages in zebrafish cell atlas [54]		
	<i>class1</i>		ENSOKIG00005022279	Expressed in macrophages [55]		
Superficial Keratinocytes	<i>ckib</i>	ENSSSAG00000003466	ENSOKIG00005016475	Expressed in monocytes [56]		
	<i>mitfa</i>	ENSSSAG00000077659	ENSOKIG00005012208	Associated with melanophores [57]		
	<i>csf1r</i>	ENSSSAG00000047020				
Intermediate Keratinocytes	<i>cxpla</i>	ENSSSAG00000048370	ENSOKIG00005025303	Expressed in mouse suprabasal keratinocytes [58]		
	<i>ppl</i>	ENSSSAG00000003101	ENSOKIG00005024627	Expressed in mouse suprabasal keratinocytes [58]		
Basal Keratinocytes	<i>clov6</i>	ENSSSAG00000074658	ENSOKIG00005006494	Facilitates lipid metabolism in human skin keratinocytes [59]		
	<i>ass1</i>	ENSSSAG00000053906	ENSOKIG00005029918	Expressed in mouse keratinocytes [60]		
Fibroblasts (1)	<i>pof1b</i>	ENSSSAG00000040788	ENSOKIG00005024403	Expressed in human keratinocytes [61]		
	<i>itga6</i>	ENSSSAG00000067255	ENSOKIG00005047168	Expressed in basal epidermal cells in humans [62]		
Endothelial	<i>lamt4</i>	ENSSSAG00000106537	ENSOKIG00005007077	Marker for "fin basal cells" in zebrafish cell atlas [54]		
	<i>fnb2b</i>	ENSSSAG00000057875	ENSOKIG00005007419	Associated with fibroblast-driven wound healing in humans [63]		
	<i>col12a1</i>	ENSSSAG00000070858	ENSOKIG00005043212	Expressed in the fibroblasts of chick skin [64]		
	<i>egf7</i>	ENSSSAG00000083641	ENSOKIG00005048982	Associated with endothelial development – specifically blood vessels [65]		
Atlantic Salmon Only	Secretory	<i>tie1</i>	ENSSSAG00000079214	ENSOKIG00005004729	Marker for the blood vessel cell type in zebrafish cell atlas [54]	
		<i>flt4</i>	ENSSSAG00000084309	ENSOKIG00005035303	Marker for the the blood vessel cell type in zebrafish cell atlas [54]	
		<i>pcdh11</i>	ENSSSAG00000057824	ENSOKIG00005037957		
		<i>avil</i>	ENSSSAG00000084911	ENSOKIG00005031571	Associated with tuft cells [66] and expressed in a rare tuft cell-like group of cells within zebrafish intestine [67]	
		<i>pou2f3</i>	ENSSSAG00000039114	ENSOKIG00005026363	Associated with tuft cells [68] and expressed in a rare tuft cell-like group of cells within zebrafish intestine [67]	
	Osteoblasts	<i>proxl</i>	ENSSSAG00000039610	ENSOKIG00005019222	Associated with tuft cells [69]	
		<i>panx3</i>	ENSSSAG00000068856	ENSOKIG00005040175	Marker for osteoblasts in zebrafish cell atlas [54]	
		<i>itga10</i>	ENSSSAG00000119547	ENSOKIG00005041776	Associated with bone development [70]	
		<i>fgfr4</i>	ENSSSAG00000017777	ENSOKIG00005032151	Expressed in mouse osteoblasts [71], marker for bone in Atlantic Salmon [28]	
	Red Blood Cells	<i>hemoglobin beta</i>	ENSSSAG00000045065	ENSOKIG00005024058	Key component of red blood cells	
	Muscle	<i>casq1b</i>	ENSSSAG00000072101	ENSOKIG00005004600	Expressed in zebrafish skeletal muscle [72]	
		<i>tni2a</i>	ENSSSAG00000055259	ENSOKIG00005033031	Critical to muscle function [73]	
		<i>tn</i>	ENSSSAG00000119643		A crucial component of skeletal muscle function [74]	
	Neural Crest Cells	<i>ltk</i>	ENSSSAG00000110394	ENSOKIG00005047857	Directs multipotent neural crest cell development into pigment cells in zebrafish [57]	
		<i>miphb</i>	ENSSSAG00000055095	ENSOKIG00005009265	Marker gene for xanthophores and melanophores in zebrafish cell atlas [54]	
<i>pmp4a</i>		ENSSSAG00000044409	ENSOKIG00005022133	Expressed in iridophores [75]		
<i>fbt2</i>		ENSSSAG00000080837	ENSOKIG00005031455	Expressed in iridophores [76]		
			ENSOKIG00005012190			
Neuronal (1)	<i>als4b</i>	ENSSSAG00000112316	ENSOKIG00005008266	Expressed in iridophores [77]		
	<i>nval1</i>	ENSSSAG00000047318	ENSOKIG00005015132	Associated with neuron development in mice [78]		
Neuronal (2)	<i>cnm4</i>	ENSSSAG00000057173	ENSOKIG00005044284	Associated with neuron development in humans [79]		
	<i>sam12</i>	ENSSSAG00000118720	ENSOKIG00005014439	Linked to neurological disease in humans [80]		
	<i>il10rb</i>	ENSSSAG00000038884	ENSOKIG00005025589	Expressed in neurons [81]		
Atlantic Salmon Only	Fibroblasts (2)	<i>lamc1</i>	ENSSSAG00000080380		Expressed in mouse fibroblasts [82]	
		<i>col6a6</i>	ENSSSAG00000040824		Expressed in human skin fibroblasts [83]	
	Mucous	<i>fer1f4</i>	ENSSSAG00000075250		lncRNA associated with gastric cancer [84]	
		<i>spdef</i>	ENSSSAG00000074163		Critical to mucus cell differentiation [85]	
		<i>p2rx1</i>	ENSSSAG00000039817		Marker for mucus cells in zebrafish cell atlas [54]	
	Glial (1)	<i>nuc3bl</i>	ENSSSAG00000055014		Associated with mucus cells [86]	
		<i>abg1</i>	ENSSSAG00000074663		Expressed in glial but also neuronal cells [87]	
Undifferentiated	<i>wdr49</i>	ENSSSAG00000064639		Associated with astrocytes [88]		
	<i>nax7l</i>	ENSSSAG00000060652		Associated with myoskeleton [89]		
Coho Salmon Only	Mucous (1)	<i>col4a1</i>	ENSSSAG00000029801		Widely expressed in basement membrane [90]	
		<i>fer1f4</i>		ENSOKIG00005027833	lncRNA associated with gastric cancer [84]	
		<i>spdef</i>		ENSOKIG00005000031	Critical to mucus cell differentiation [85]	
		<i>p2rx1</i>		ENSOKIG00005008860	Marker for mucus cells in zebrafish cell atlas [54]	
	Mucous (2)			ENSOKIG00005028810		
		<i>fer1f4</i>		ENSOKIG00005027833	lncRNA associated with gastric cancer [84]	
		<i>spdef</i>		ENSOKIG00005003413	Critical to mucus cell differentiation [85]	
	Integument	<i>p2rx1</i>		ENSOKIG00005028810	Marker for mucus cells in zebrafish cell atlas [54]	
		<i>plcb2</i>		ENSOKIG00005013873	Marker for "Integument – taste bud" cell type in zebrafish cell atlas [54]	
		<i>rgs1</i>		ENSOKIG00005032617	Marker for "Integument – taste bud" cell type in zebrafish cell atlas [54]	
				ENSOKIG00005021878	Marker for "Integument – taste bud" cell type in zebrafish cell atlas [54]	
		<i>trpm5</i>		ENSOKIG00005033333	Marker for "Integument – taste bud" cell type in zebrafish cell atlas [54]	
	Neuronal (3)	<i>kcnk17</i>		ENSOKIG00005039197	Marker for "Integument – taste bud" cell type in zebrafish cell atlas [54]	
		<i>alk</i>		ENSOKIG00005020768	A widely-expressed neuronal-related gene [91], also associated with pigmentation in fish [92]	
	Glial	<i>abg1</i>		ENSOKIG00005034390	Expressed in glial but also neuronal cells [87]	
<i>wdr95</i>			ENSOKIG00005007677	An ortholog of WDR49, which is associated with astrocytes [88]		

The integration of samples from both species demonstrated the majority of cell types observed in each of the species-specific datasets (Fig. 2a, see Additional file 2 for all detected marker genes). Two clusters of immune cells were uncovered in the combined dataset which we designated “lymphocyte” and “myeloid” given their expression of *itgae* [94] and *cd163* [95], respectively. The marker genes for each cluster of the combined dataset were often identical to those marker genes in the corresponding cluster in the species-specific dataset and always highly expressed (Fig. 2b, c, d), confirming the presence of identical cell types in the skin of Atlantic salmon and coho salmon. However, the species-specific datasets presented additional clusters and had a greater number of marker genes given more genes were used in the clustering (salmonids present a recent whole-genome duplication and the

establishment of 1:1 orthologs are not straightforward, which resulted in many genes being removed when the datasets of the two species were combined). Therefore, all further analyses were conducted using the species-specific datasets, which we refer to exclusively from this point forward.

Non-immune cell types

Keratinocytes were among the most abundant cell types. Three keratinocyte clusters were identified: basal keratinocytes, superficial keratinocytes, and a third cluster of “intermediate keratinocytes”, likely located between the former two keratinocyte layers and consistent with the three layers of keratinocytes observed in fish skin [30, 31]. Keratinocytes were abundant in all samples, but notably increased at 48 h and 60 h post infection only in coho salmon (Fig. 1e, f).

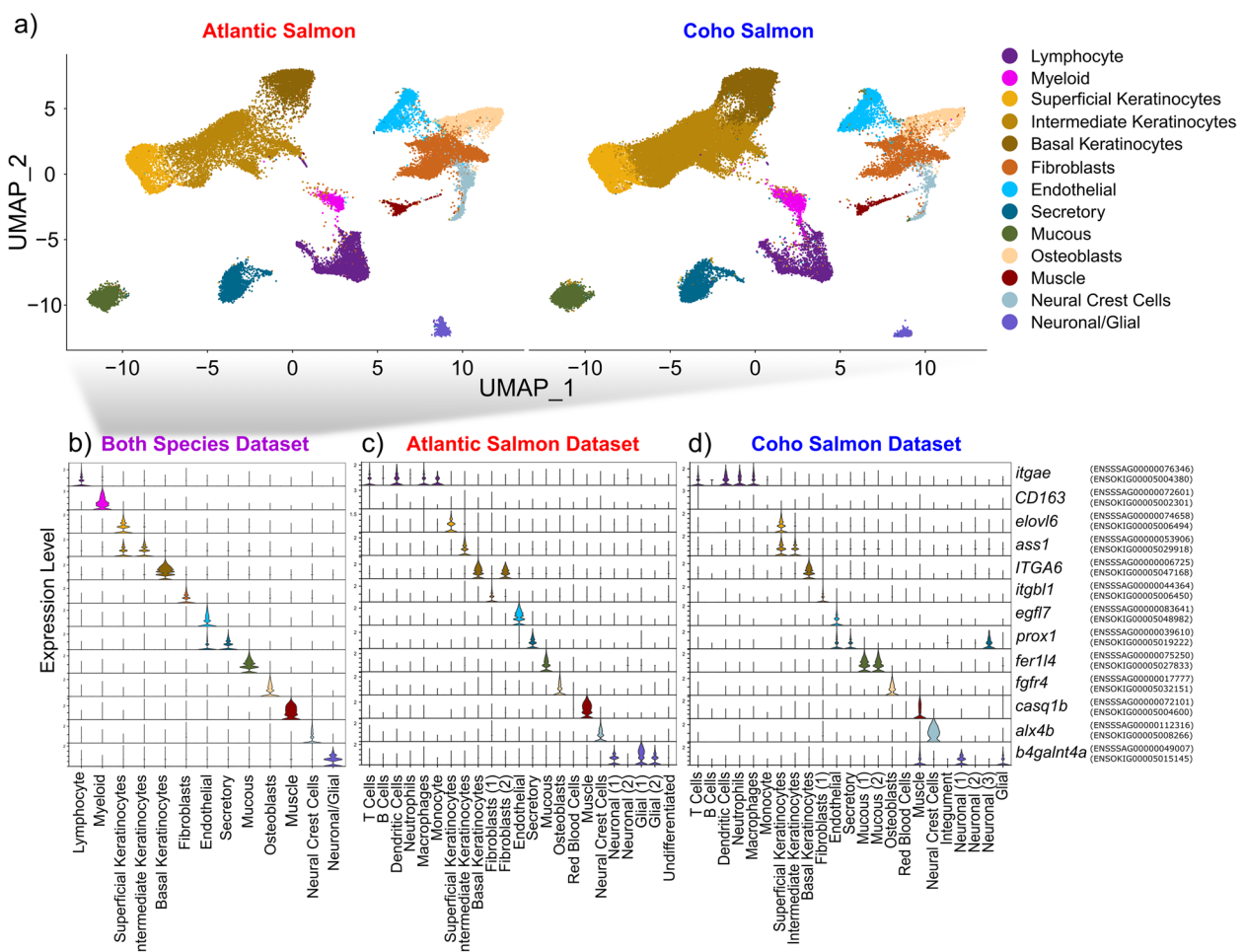


Fig. 2 Cell clusters identified integrating both Atlantic salmon and coho salmon samples using 1:1 orthologous genes. **a** UMAP of cell clusters split by species, **b** violin plot of expression of a marker gene for each cluster. Violin plots visualize the expression of these same features in the species-specific datasets: **c** Atlantic salmon, **d** coho salmon. The Atlantic salmon and coho salmon ortholog Ensembl codes are noted to the right of each gene

Other abundant cell types include fibroblasts, endothelial cells, and osteoblasts. Mucous cells were split into two clusters in coho salmon with many overlapping markers (Additional file 1: Figs. S5, S6), but differing in their relative expression of different paralogs of *spdef* and *p2rx1* (see Additional file 1: Figs. S2, S5, S6). Interestingly, *muc5* (associated with mucous cells [86]) was expressed only in Atlantic salmon mucous cells (Additional file 1: Figs. S1, S2). A “secretory” cell type was abundant in both species and expressed tuft-cell marker genes (Table 1). Tuft cells line the epithelium of the gut and airway in mammals, and although their function is not well-characterized, they are associated with initiating immune responses (e.g. activating Th2 cells in response to helminth endoparasitism in mice) [96]. We speculate these may be a sacciform cell type, previously noted in coho salmon [21]. However, the noted absence of sacciform cells in Atlantic salmon [21] means that the location, morphology, and function of this newly identified cell type requires further investigation.

Neural crest cells were characterized by multiple pigment cell genes (Table 1) including *ltk*, which directs multipotent neural crest cell development into pigment cells in zebrafish [57], suggesting these cells are pigment cell progenitors. The detection of neural crest cells, red blood cells, and muscle cells predominately in trunk skin samples (Fig. 1e, f) is consistent with expectations of greater abundance of these cell types in the trunk skin than in the fins [31] given the potential to cut deeper into the dermal layer. Additionally, several clusters of neuronal and glial cells were observed, but most were observed in a single sample per species (Fig. 1e, f) suggesting they comprise neural structures which are present sporadically throughout the skin (e.g. peripheral axons [35] or the lateral line). Given their inconsistent presence within our samples, we do not further consider the response of these cell types to sea lice, but note their potential to confound bulk RNAseq skin data.

Several cell types were identified in only one species. A small cluster of cells detected in coho salmon demonstrated a number of marker genes observed in cluster 196 “Integument-Taste Bud” of a zebrafish cell atlas [54] (Table 1), which we refer to as “integument” cells henceforth. We speculate this cell cluster may represent a rare chemosensory cell type in coho salmon, which may also be present in Atlantic salmon but was unobserved due to its rarity ($N=93$ cells in coho salmon). Fibroblasts (2) were detected in Atlantic salmon but not coho salmon and expressed *lamc1* and *col6a6* but also marker genes of the keratinocyte clusters (e.g. *itga6* and *pof1b*) (Additional file 1: Fig. S1). A final cell cluster unique to Atlantic salmon was termed “Undifferentiated” because of its few distinctive marker genes (Additional file 1: Figs. S1, S7).

Immune cell types

The immune cell marker gene *cd45* [97] was expressed in four and two clusters for Atlantic salmon and coho salmon, respectively (Additional file 1: Fig. S8). These clusters were reclustered to investigate for additional immune cell types expected to be present in the skin and potentially involved in sea lice response [19]. Substructuring within *cd45+* cells revealed six main types of immune cells in both species: T cells, B cells, dendritic cells, neutrophils, macrophages, and monocytes (Fig. 3a, b). Myeloid and lymphocyte cells were clearly differentiated by the expression of *spi1b*, a marker for the myeloid lineage in zebrafish [40]. Marker genes for all immune cell types were consistent with the literature (Table 1) with the curious exception of the monocyte marker gene *mitfa*, typically associated with melanophores [57], suggesting these monocytes might develop into melanomacrophages known to be present in salmonid skin [20] (Figs. 1c, d, 3c, d, see Additional file 1: Figs. S9–S31 for violin plots of top marker genes and Additional file 2 for all marker genes).

While multiple macrophage and T cell subclusters were apparent in each species, their top marker genes were either largely overlapping among subclusters, mostly ribosomal genes, or had unknown biological relevance (Additional file 1: Figs. S9–S12, S17–S19, S21–S23, S25, S29–S30), suggesting these are clustering artefacts or previously undescribed immune cell types. For instance, expression of *cd4* and *cd8* also did not conclusively differentiate T cell subclusters (Additional file 1: Fig. S32); however, T cells (5) in Atlantic salmon (Additional file 1: Fig. S13) and T cells (4) in coho salmon (Additional file 1: Fig. S24) expressed *gata3*, associated with Th2 cell activation [98]. Given this general lack of clear, biologically relevant expression differences within T cell and macrophage subclusters, and to maximize power for subsequent differential expression analyses (given the low numbers of cells in each T cell and macrophage subcluster, Additional file 1: Tables S6, S7), we grouped together all T cell subclusters and all macrophage subclusters for downstream analysis.

Common responses to sea lice in resistant and susceptible salmonid species

A total of 4567 and 1799 unique genes were found to be differentially expressed between any treatment time point and the control in Atlantic salmon and coho salmon, respectively (see Additional file 1: Figs. S33–S35 for the distribution of differentially expressed genes within a given cell type, see Additional file 1: Figs. S36, S37 for GO enrichment results, see Additional file 2 for all differentially expressed genes). Some conserved wound-healing

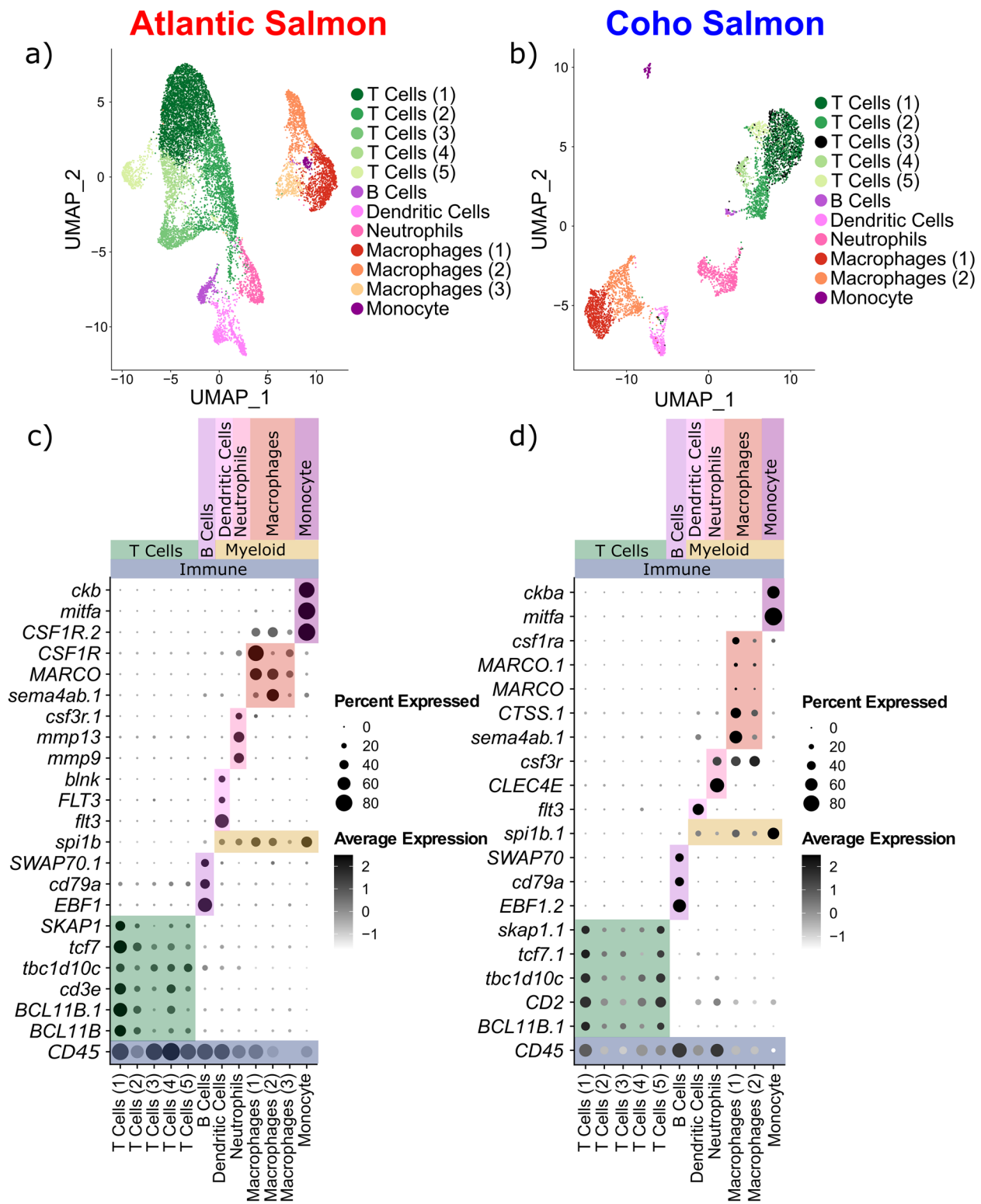


Fig. 3 Sub-clustering of putative immune cells expressing *CD45*. UMAP visualization of immune clusters in Atlantic (a) and coho (b) salmon. Dot plots of features characterizing immune cell types in Atlantic (c) and coho (d) salmon

and immune responses to sea lice infection were detected in Atlantic salmon and coho salmon.

Wound-healing response to sea lice

Both species showed a clear activation of wound-healing mechanisms in response to the parasite in a variety of cell types (Fig. 4). Upregulation of genes linked to limb development such as *pax9* [99] and *meis2* [100] were evident in keratinocytes, mucous cells, and/or fibroblasts. Genes associated with extracellular matrix integrity including *pdgfra* [101] and *col21a* [102] were upregulated in fibroblasts of both species. Another gene associated with healing of individual cells, *abr* [103], was significantly upregulated in macrophages and T cells in coho salmon and in mucous cells, keratinocytes, and T cells in Atlantic salmon. The upregulation of *agr2* observed in mucous cells of both species probably reflects an increased production of mucus in response to sea lice [104] potentially to aid in wound healing [31, 93]. A gene previously found to be upregulated at louse attachment sites in Atlantic salmon [105], *aloxe3*, was upregulated in mucous cells of both species but only significantly in Atlantic salmon. Mutations to *aloxe3* are associated with ichthyosis, a condition resulting in the build-up of skin cells [106], suggesting this gene could contribute to wound-healing-associated cell growth. Similarly, epidermal reinforcement-related genes *cldn8* [107] and *cntr1* [108] were more upregulated in Atlantic salmon. However, *bnc2*, associated with wound healing and fibrosis [109], as well as black pigmentation [110], was upregulated earlier and more strongly in coho salmon basal keratinocytes. Similarly, *hpse2*, associated with cell proliferation and extracellular matrix strengthening [111], was upregulated in coho salmon fibroblasts but downregulated in Atlantic salmon fibroblasts. Therefore, while general wound-healing mechanisms are activated in both species, differences can be detected.

Immune response to sea lice

A clear immune response was observed in both species in response to sea lice (Fig. 5). Multiple paralogs of genes associated with immune cell development including *runx3* [112], *rarb* [113], and *gnai2* [114] were upregulated in response to sea lice in a variety of immune cell types including T cells, macrophages, and dendritic cells (Fig. 5a). *Myo9b*, a gene associated with immune cell motility and activation [115], was upregulated in dendritic cells, neutrophils, and macrophages in both species, though showing a faster and more intense upregulation in coho salmon (Fig. 5a). Major histocompatibility components were significantly upregulated in macrophages and T cells (*MHCII* only) but surprisingly in non-immune cell types too, mainly keratinocytes,

and particularly superficial keratinocytes (Fig. 5b). The involvement of the complement immune system was unclear. Two paralogs of *c4* were upregulated in Atlantic salmon fibroblasts while in coho salmon fibroblasts, one paralog was not differentially expressed, and the other was upregulated at 24 h but downregulated at 36 h and 60 h (Fig. 5c). *Cfd* was significantly downregulated in Atlantic salmon fibroblasts but was not significantly differentially expressed in coho salmon (Fig. 5c). This is consistent with previous observations of the downregulation of this gene in Atlantic salmon in response to *L. salmonis* sea lice [105]. Though Atlantic salmon demonstrated robust activation and differentiation of T cells through the significant upregulation of *cd28*, *ifit9*, *sox4* [116], *cxc4* [117], and *ly-9* [118], they also significantly upregulated anti-inflammatory *socs3* [119] (Fig. 5d).

Responses to sea lice unique to coho salmon

Downregulation in coho salmon red blood cells in response to sea lice

Atlantic salmon red blood cells upregulated a number of genes associated with iron binding including several haemoglobin and ferritin subunits, and *tfr1a* [120] and other genes key to red blood cell function including *slc4a1a* (ion transportation [121]) and *alas2* (heme biosynthesis [26]) (Fig. 6a). On the contrary, there was a significant downregulation of these genes in coho salmon red blood cells (Fig. 6a). A regulation of iron in coho salmon red blood cells was further supported by the enrichment of a variety of iron-related GO terms (e.g. iron ion transport—GO:0006826) in sea louse infected samples of coho salmon but not Atlantic salmon (Fig. 6b).

Keratinocytes are key to epithelial hyperplasia response to sea lice in coho salmon

A variety of genes associated with epidermal re-organization were exclusively and significantly upregulated in coho salmon keratinocytes (Fig. 7a, b). Keratinocytes in both species were enriched for intermediate filament cytoskeleton organization (GO:0045104) and intermediate filament-based process (GO:0045103), consistent with the known abundance of filaments observed in salmon keratinocytes [29] (Fig. 7c). However, the fold enrichment was much higher in coho salmon, indicating greater cell movement and restructuring of keratinocytes in this species (Fig. 7c).

Coho salmon superficial keratinocytes expressed genes more associated with cell motility and immune cell localization, consistent with their location in the outermost layer of the epidermis and in direct contact with attached lice [31] (Fig. 7b). The GO term epidermis development (GO:0008544) was enriched in coho salmon superficial keratinocytes and to a lesser extent in

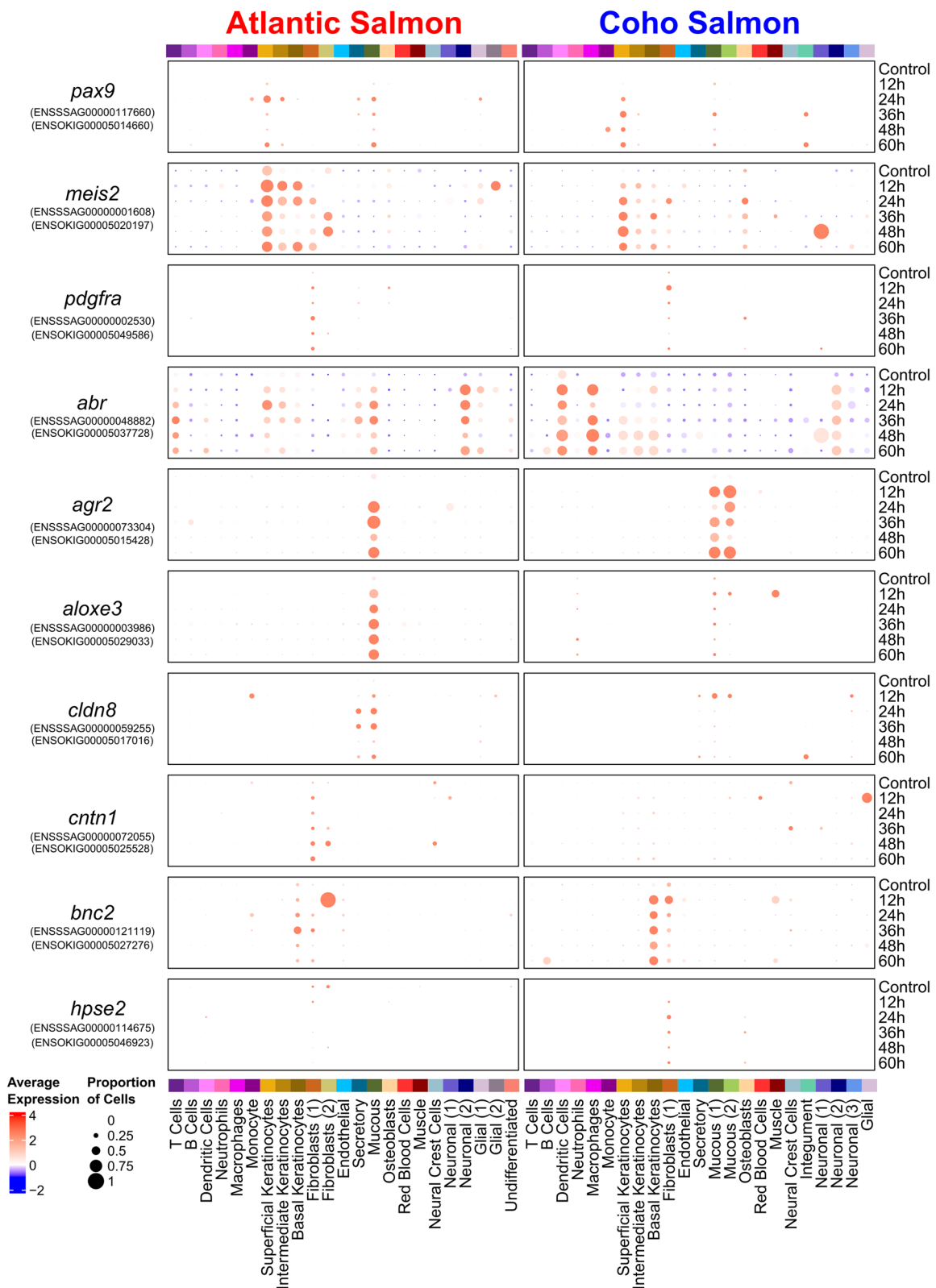


Fig. 4 Dot plots of wound healing-related gene expression in Atlantic salmon and/or coho salmon in response to sea lice. All genes shown were significantly differentially expressed ($p_{adj} < 0.001$) in at least one pairwise comparison between the control and any treatment time point in either species

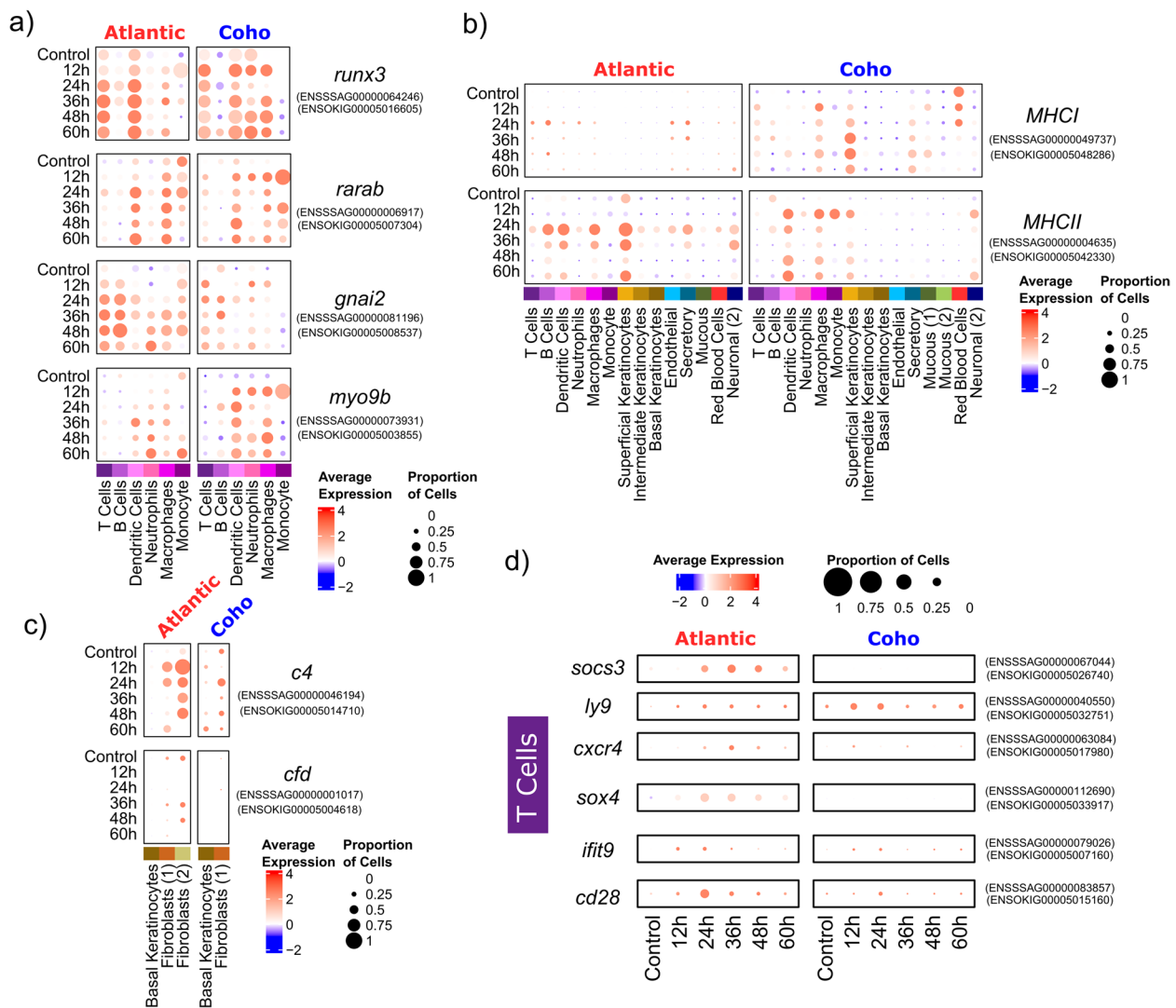


Fig. 5 Dot plots of immune-related gene expression in Atlantic salmon and/or coho salmon in response to sea lice. **a** Immune genes upregulated in both species, **b** MHC genes upregulated in both species, **c** complement immune system gene expression, **d** immune-related genes particularly upregulated in Atlantic salmon in response to sea lice. All genes shown were significantly differentially expressed ($p_{\text{adj}} < 0.001$) in at least one pairwise comparison between the control and any treatment time point in either species

intermediate keratinocytes (Fig. 7c). Increased cell motility in coho salmon superficial keratinocytes and intermediate keratinocytes was also evident by the increased expression of *glipr2*, associated with cell migration particularly in response to hypoxia [122], and *egfra*, associated with epidermal cell proliferation [123] (Fig. 7a). Coho salmon superficial keratinocytes also upregulated genes related to inflammation and immune cell infiltration including *sat1* [124], *spns2* [125], and *cdh26* [126] (Fig. 7a).

In contrast, the basal keratinocyte response in coho salmon was characterized by the upregulation of genes associated with extracellular matrix reinforcement,

consistent with their location in the outermost layer of the dermis [31] (Fig. 7b). Genes associated with cell adhesion and the extracellular matrix including *plecb* [127] and *mmp30* [128] were significantly upregulated in coho salmon (Fig. 7a). GO terms associated with extracellular matrix development (e.g. cell-cell adhesion via plasma-membrane adhesion molecules—GO:0098742, and cell adhesion—GO:0007155, which is also enriched in intermediate keratinocytes) were also significantly enriched in coho salmon basal keratinocytes (Fig. 7c). This layer of keratinocytes may also be responsible for directing the movement of upper layers of keratinocytes through the upregulation of genes known to regulate cell motility

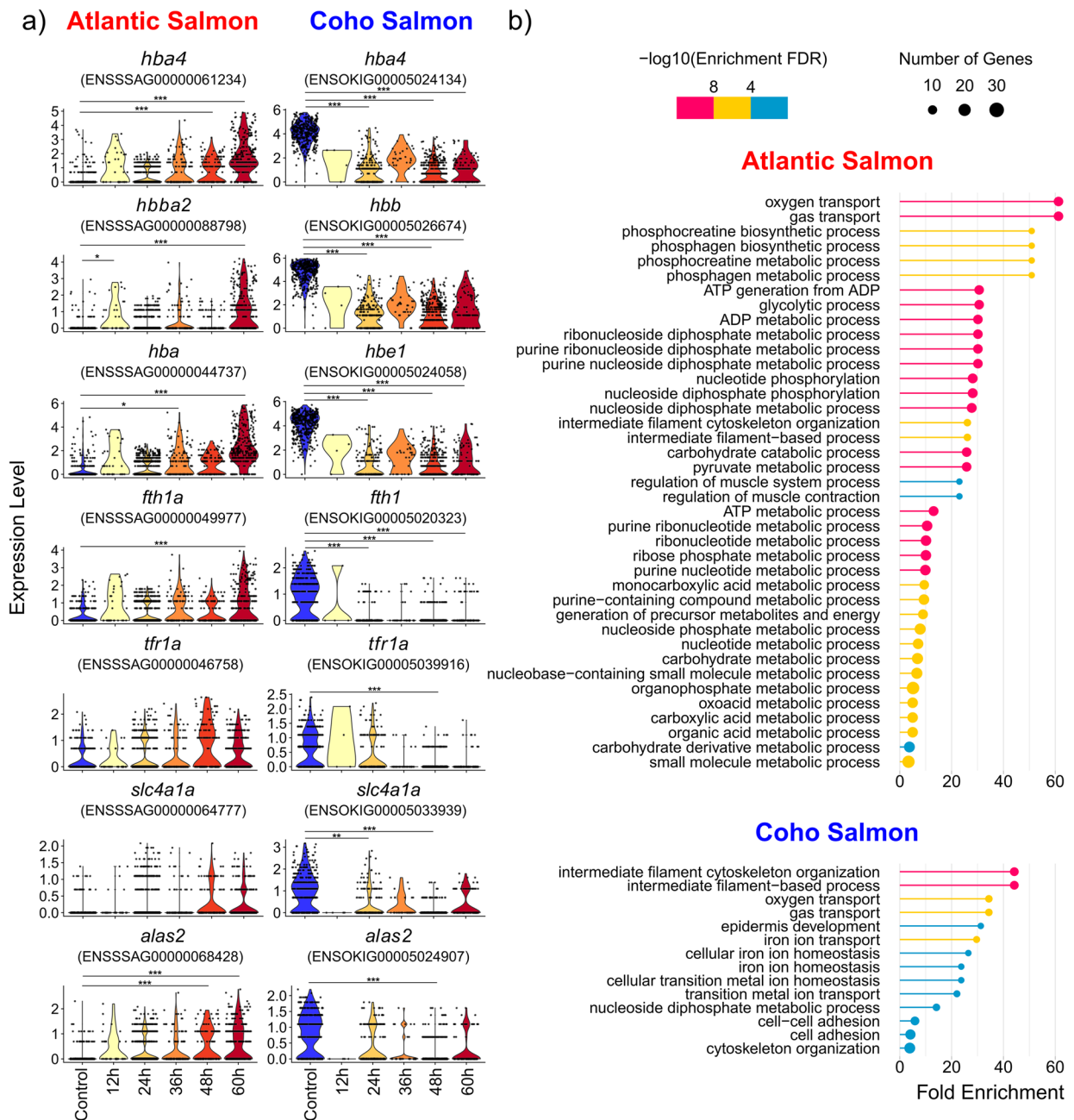


Fig. 6 Red blood cell response to sea lice in Atlantic salmon and coho salmon. **a** Violin plots of gene expression in Atlantic salmon and coho salmon of genes significantly upregulated in coho salmon keratinocytes ($p_{\text{adj}} < 0.001$) in response to sea lice in at least one treatment time point relative to the control (*— $p_{\text{adj}} < 0.001$, **— $p_{\text{adj}} < 0.0001$, ***— $p_{\text{adj}} < 0.00001$), **b** significantly enriched biological GO terms ($p_{\text{adj}} < 0.001$) for red blood cells in response to sea lice in Atlantic salmon and coho salmon

including *plekhgb5b* [129] and *quo* [130] (Fig. 7a) and supported by the significant enrichment for GO:0032231, regulation of actin filament bundle assembly (Fig. 7b, c). Coho salmon basal keratinocytes also upregulated the immune gene *jak2a* (Fig. 7a), which regulates haematopoiesis [131], promotes cell proliferation [132], and

is inhibited by *socs3* [133] (upregulated only in Atlantic salmon (Fig. 5d)). An aerolysin-like protein, which breaks down cell membranes [134] and is upregulated in fish in response to bacterial infections (e.g. [135, 136]), was also significantly upregulated exclusively in coho salmon basal keratinocytes (Fig. 7a), confirming earlier observations

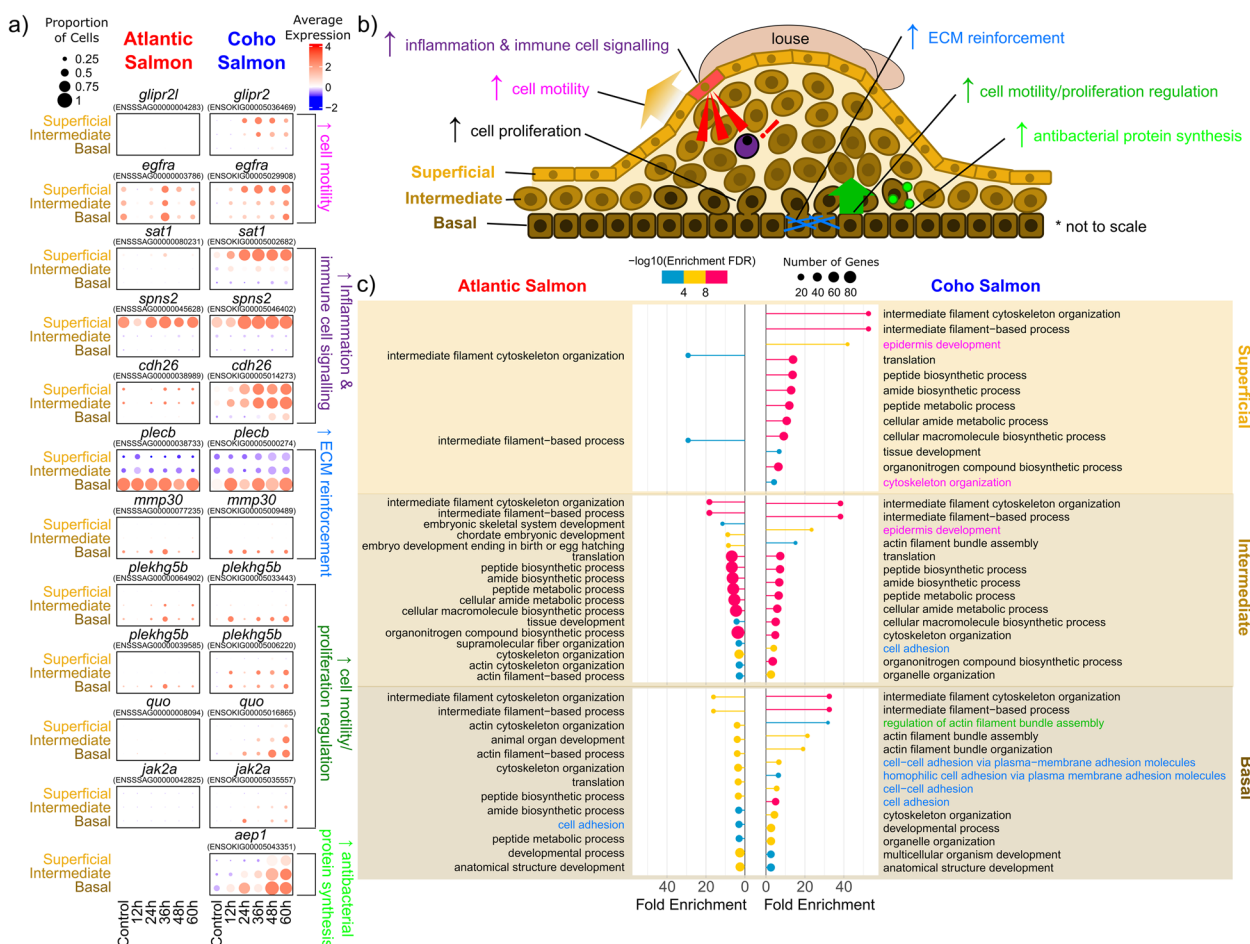


Fig. 7 Keratinocyte response to sea lice underlies coho salmon resistance to sea lice. **a** Dot plots of gene expression in Atlantic salmon and coho salmon of genes significantly upregulated in coho salmon keratinocytes ($p_{adj} < 0.001$) in response to sea lice in at least one treatment time point relative to the control. **b** proposed unique contributions of superficial, intermediate, and basal keratinocytes to epithelial hyperplasia immune response to sea lice in coho salmon, **c** significantly enriched biological GO terms ($p_{adj} < 0.001$) for superficial, intermediate, and basal keratinocytes in response to sea lice in Atlantic salmon and coho salmon. Differentially expressed genes in **a** and GO terms in **c** are colour-coded by the biological processes depicted in **b** that they are potentially associated with

of the upregulation of this gene exclusively in the skin of coho salmon but not of Atlantic salmon in response to sea lice [24].

The differentially expressed genes characterizing the intermediate keratinocytes' response to sea lice in coho salmon largely overlapped with either the basal or superficial keratinocytes (Fig. 7a). This less specialized role is consistent with their location between the superficial and basal keratinocytes. It may also reflect their recent generation from basal keratinocytes [137] as evidenced by the particular increase in abundance of this layer of keratinocytes at 48–60 h (Fig. 1f).

Other cell types potentially contributing to coho salmon epithelial hyperplasia in response to sea lice

Several additional cell types express genes related to inflammation in coho salmon (Fig. 8). Secretory cells

significantly upregulated *ttc7a* from 24 h onward in coho salmon but this gene was only significantly upregulated at 36 h in Atlantic salmon. This gene is associated with epithelial inflammation in mice [138]. Alternatively, *mrc1*, a gene linked to inflammation [139] and associated with increased *C. rogercresseyi* sea lice count on Atlantic salmon [140], was significantly upregulated in coho salmon but not Atlantic salmon endothelial cells. Coho salmon macrophages also demonstrated upregulation of the inflammation-associated gene *usp47* [141]. Multiple cell types may therefore potentially regulate the keratinocyte epithelial hyperplasia response to sea lice observed in coho salmon.

Discussion

Our results suggest that Atlantic salmon and coho salmon skin share a common set of cell types consistent with their recent divergence 30 million years ago [142].

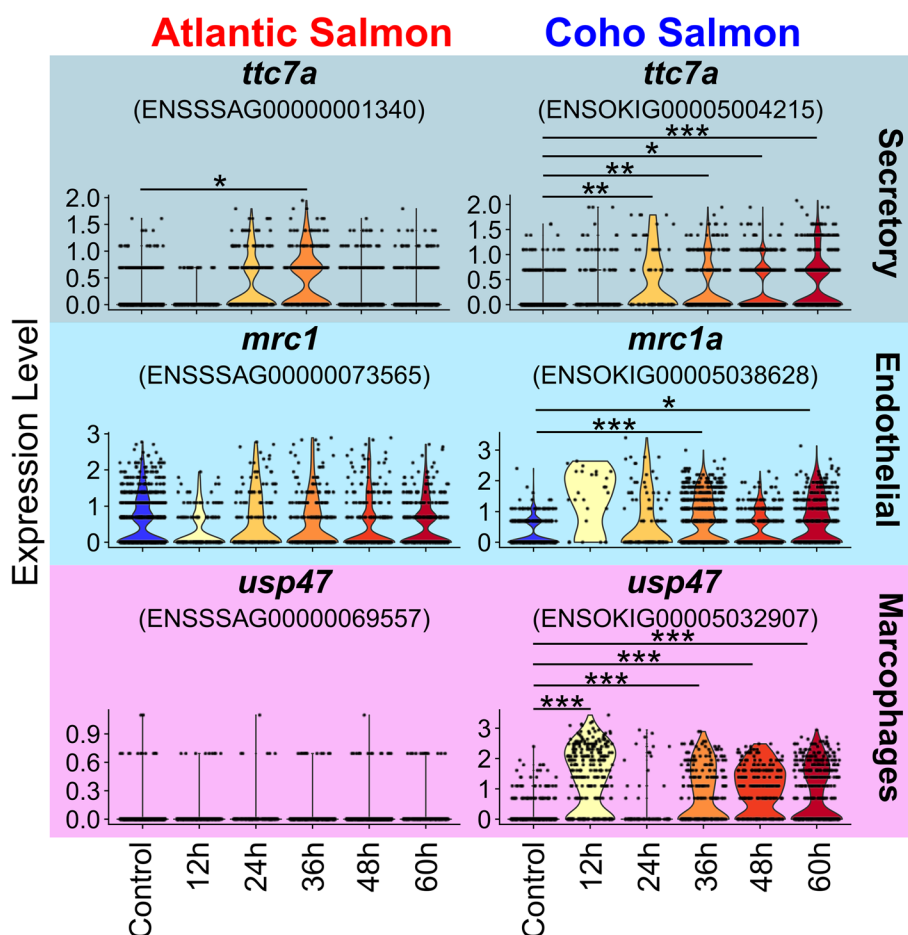


Fig. 8 Violin plots of gene expression in Atlantic salmon and coho salmon in response to sea lice that are potentially regulating coho salmon's epithelial hyperplasia response to sea lice. The cell type for which the expression of each gene is shown is noted to the right of each plot (*— $p_{\text{adj}} < 0.001$, **— $p_{\text{adj}} < 0.0001$, ***— $p_{\text{adj}} < 0.00001$.)

Many of these cell types demonstrate a clear response to sea lice, which includes the activation of wound-healing and immune mechanisms, often common to both species. Conversely, lice immunomodulation of a variety of cell types was evident only in Atlantic salmon. Additionally, the coho salmon response to sea lice presented unique signatures, characterized by iron limitation in red blood cells and a dramatic stimulation and re-organization of keratinocytes. These processes are likely to be major contributors to this species' resistance to sea lice, and the underlying genes and regulatory networks detected here are potential candidates whose expression and functioning could be disrupted to "rewire" the host response to sea lice in Atlantic salmon via biotechnological approaches such as gene editing [17].

Wound-healing response

Both species appear to employ a common wound-healing response to sea lice using a combination of

keratinocytes, fibroblasts, mucous cells, and immune cells, in agreement with the critical role of these cell types in response to skin laceration [93]. The expression of limb development-related genes in multiple cell types also confirms a large-scale rearrangement of the skin in response to wounding [31]. Fibroblastic repair of the dermis, as expected shortly after wounding [31], was also evident through the upregulation of genes related to extracellular matrix reconstruction in fibroblasts in both species. Mucous cell upregulation of *abr2* also suggests both species increased mucus production in response to sea lice. Though sea lice feed on mucus [143], increased mucus production is a characteristic wound-healing response in Atlantic salmon [31, 93]. Alternatively, mucus upregulation may be particularly adaptive in coho salmon since, unlike Atlantic salmon, mucus of this species does not prompt a protease increase from sea lice, suggesting coho salmon mucus may contain protective qualities [144].

Immune response

Both species mount a common immune response to sea lice invoking the innate, adaptive, and complement immune systems. The upregulation of major histocompatibility proteins in the skin of both species is consistent with previous observations [25, 145]. Our results suggest that the expression of *MHCII* is not limited to immune cell types, but is also evident in the superficial keratinocytes. This is consistent with similar observations of *MHCII* expression in human keratinocytes [146, 147] and may explain previous observations of *MHCII* expression in Atlantic salmon epidermis in response to sea lice [25, 148]. Our results support the potential importance of superficial keratinocytes for sensing pathogens via antigen presentation and initiating immune and inflammatory responses [149].

Similarly, keratinocytes and fibroblasts seem to be key to the activation of the complement immune system. However, our results do not provide clear support for the importance of the complement immune response to sea lice resistance. This is consistent with previous observations of both the upregulation [140, 150] and downregulation [105] of complement proteins in Atlantic salmon in response to sea lice. Our results therefore support earlier suggestions that activation of the complement pathway may not be sufficient to grant sea lice immunity in Atlantic salmon [140].

Our results also potentially indicate that Atlantic salmon and coho salmon preferentially employ different immune cells in response to sea lice. Atlantic salmon had far more T cells than coho salmon (Fig. 1e, f) perhaps as a consequence of artificial selection with selective breeding for disease resistance in this aquaculture strain of Atlantic salmon [151]. Similar artificial selection for higher numbers of T cells in coho salmon is not likely given that the coho families were derived from parents stripped of egg and milt soon after capture from the wild.

Atlantic salmon also demonstrated greater upregulation of genes associated with T cell activation. This observation may be partly attributable to differences in power among species to detect differential expression in T cells but is consistent with previous evidence suggesting a T cell dominated response to sea lice in Atlantic salmon [152]. In contrast, coho salmon potentially show a greater use of their macrophages in response to sea lice, as evidenced by the significant enrichment for “antigen processing and presentation” (GO:0019882) in coho salmon but not Atlantic salmon macrophages. Our results also support the key role of macrophages in directing coho salmon skin inflammation in response to sea lice [18], specifically through the upregulation of *usp47* and *ndst1a*, genes which are both associated with macrophage-driven inflammation [141, 153]. We

speculate that coho salmon employ a macrophage-dominant innate immune response to sea lice, while Atlantic salmon try (and fail) to employ a T cell-led adaptive immune response. For example, Atlantic salmon may be employing a maladaptive regulatory T cell-mediated dampening of the non-specific antigen response in a failed attempt to avoid immunopathology [154]. More sampling or targeted snRNA sequencing of immune cells, allowing for greater power to detect cell type heterogeneity within macrophages and T cells, as well as cytokine signalling among immune cell types, could be helpful to test this hypothesis.

Given the known importance of neutrophils to wound healing [31] and previous observations of a greater abundance of neutrophils at the site of sea lice in both species [18], the seeming lack of response in neutrophils to sea lice attachment in either species in this study was surprising. Few differentially expressed genes were observed in this cell type and no GO terms were enriched for either species, likely a result of low power due to the few neutrophils detected in each species. Genes identified in this study as markers for neutrophils (e.g. *mmp9*, *mmp13*, *csf3r*) have also been observed to be upregulated at the site of sea lice attachment in both species (e.g. [23, 155]). This discrepancy may reflect a true relative rarity of neutrophils in comparison to other skin cell types (e.g. keratinocytes and fibroblasts which dominated our samples). Alternatively, this may be a sampling bias due to the demonstrated difficulty in capturing this cell type with scRNAseq [156]. More sampling, adjustment of nuclei isolation protocols to target delicate granulocytes, or integration of snRNA sequencing data with spatial transcriptomic data may help to further reveal how neutrophils and other granulocytes such as eosinophils (which have also been observed at the site of sea louse attachment in coho salmon [20] but were not apparent in our data) are responding to sea lice.

Potential immunomodulation of Atlantic salmon by sea lice

Given the known susceptibility of Atlantic salmon to sea louse immunomodulation [157, 158], differences in immune and wound-healing response between Atlantic salmon and coho salmon may not only reflect host physiological differences but also the differential capacity of sea lice to immunomodulate each species. For example, we speculate that the upregulation of the inflammation-dampening *socs3* [119] in Atlantic salmon T cells may be a result of sea louse immunomodulation. This gene is also upregulated in Atlantic salmon skin and head kidney in response to *C. rogercresseyi*, but is downregulated when Atlantic salmon are fed an immunostimulatory diet associated with lower lice counts, suggesting

that this upregulation in response to *C. rogercresseyi* is maladaptive [159]. *Socs* genes are commonly targeted by fish pathogens to dampen host immunity [160] and may be particularly effective at preventing macrophage activation (e.g. in turbot in response to bacterial pathogens [161]). In combination with these earlier observations, our results therefore suggest that *L. salmonis* may strategically induce *socs3* upregulation in Atlantic salmon to weaken their hosts. However, given the potential of *socs3* to both improve or worsen pathology to specific diseases given its involvement in multiple immune system regulatory pathways [119], it is also possible that differences in *socs3* expression among coho and Atlantic salmon could reflect differences in the host-specific immune response irrespective of sea lice-induced immune suppression. Nonetheless, further study of this gene and its role in suppressing the host immune response to sea lice, particularly among T cell types, is warranted.

Lice immunomodulation may also have caused the dampened expression of *hpse2* and *bnc2* in Atlantic salmon, potentially resulting in reduced capacity for wound healing, and, in the case of *bnc2*, melanisation [110]. Melanisation is frequently observed at the louse attachment sites in Atlantic salmon [31] and is more pronounced in Atlantic salmon with greater sea lice resistance [162]. Therefore, sea lice may downregulate *bnc2* in Atlantic salmon to prevent effective wound healing.

Upregulation of haemoglobin and ferritin in Atlantic salmon red blood cells could also reflect lice immunomodulation for the purposes of increasing the parasite's access to the host's iron. Many pathogens manipulate iron homeostasis to increase available iron both for nutritional purposes and potentially as a method of weakening their host [163, 164], as excess iron can contribute to Fenton chemistry production of harmful reactive oxygen-containing species [165]. Ferritin and genes related to heme biosynthesis have previously been observed to be upregulated in the skin of Atlantic salmon in response to *L. salmonis* [166]. This was suggested to be an adaptive compensatory response to blood loss from *L. salmonis* parasitism; however, we suggest that this may instead be a maladaptive response due to *L. salmonis* immunomodulation of Atlantic salmon. This is supported by the observation that haemoglobin is downregulated in Atlantic salmon infected with *C. rogercresseyi* when they are fed an immunostimulatory diet [159]. *L. salmonis* secretion of prostaglandin E2 or other vasodilators may underlie this response in Atlantic salmon [167]. Our results therefore suggest the potential for sea lice to manipulate a wide range of molecular pathways and phenotypes in Atlantic salmon related to immune response, wound healing, and iron availability. Additional molecular research from the perspective of the sea louse would

be useful to substantiate these findings and identify the precise molecular strategies employed by the sea louse to elicit these responses in Atlantic salmon.

Potential nutritional immune response in coho salmon red blood cells may discourage sea lice

In contrast to Atlantic salmon, coho salmon red blood cells downregulate multiple iron-binding genes in response to sea lice. This could reflect differential wound-healing strategies in each species or may potentially indicate an adaptive nutritional immune response. Nutritional immunity, where hosts reduce the availability of iron in their tissues, is commonly employed to dissuade iron-seeking pathogens [27]. Pink salmon downregulate iron-associated genes in response to sea lice [168] and a nutritional immune response resulting from the upregulation of *hepcidin 1* has been suggested for both Atlantic salmon and coho salmon [25]. However, we found low expression of *hepcidin* in both species in all samples. Instead, our results suggest that this nutritional immune response in coho salmon is derived from the downregulation of a variety of iron-binding genes in red blood cells.

Atlantic salmon, however, are nevertheless clearly capable of mounting a similar nutritional immune response to other pathogens. For example, plasma iron significantly decreased in Atlantic salmon exposed to live and dead *Piscirickettsia salmonis* bacteria [120]. Intriguingly, Atlantic salmon seem capable of mounting a similar nutritional immune response by upregulating genes associated with heme degradation when parasitized by *C. rogercresseyi* but not *L. salmonis* [166]. *L. salmonis*' longer co-evolutionary history with Atlantic salmon [169] may have resulted in its greater capacity to immunomodulate Atlantic salmon in comparison to *C. rogercresseyi*. Given the susceptibility of Atlantic salmon to both sea louse species, restoring Atlantic salmon's adaptive nutritional immunity may not be sufficient to confer resistance to *L. salmonis*. However, this may still result in positive animal welfare consequences given that iron limitation can prevent opportunistic microbial infections [170] that are often associated with the sites of sea lice attachment [171].

Keratinocytes key to coho salmon epithelial hyperplasia immune response to sea lice

Our results strongly suggest that keratinocytes are responsible for the epithelial hyperplasia response characterized by filament development, inflammation, and cell proliferation that coho salmon employ to expel sea lice [18, 19, 22]. This is evidenced by our observations of a significant upregulation of genes associated with cell proliferation, cell motility, and extracellular matrix strengthening in keratinocytes, in addition to their

dramatic increase in abundance during sea lice infection. However, our results further reveal keratinocytes play an active immunological role in response to sea lice. Given their capacity for antigen presentation through the expression of *MHCII*, superficial keratinocytes may play a sentinel role in the detection of sea lice and subsequently attract immune cells to the site of an attached sea louse. Superficial keratinocytes and to a lesser extent intermediate keratinocytes also seem to be responsible for the dramatic increase in filament cell proliferation typifying coho salmon response to sea lice [18, 19] as evidenced by their upregulation of genes related to cell motility and filament reorganization. The intermediate keratinocytes, which we suggest lie between the superficial and basal keratinocytes due to their shared marker and differentially expressed genes, rapidly increase in abundance at 48–60 h post sea lice infection and are likely responsible for the observed skin thickening in coho salmon in response to sea lice [18, 19]. Basal keratinocytes, alternatively, regulate the cell motility and proliferation of the upper layers of keratinocytes, strengthen the basement membrane of the epidermis, and produce antibacterial aerolysin proteins to prevent secondary microbial infections. Therefore, each layer of keratinocytes plays a unique but integrated role in the observed epithelial hyperplasia characterizing coho salmon's response to sea lice.

Conclusions

In this study, we revealed the cell-specific mechanisms underlying responses to sea lice in a susceptible and a resistant salmonid species. Single-nuclei RNA sequencing allowed us to identify the importance of genes with cell type-specific expression patterns, and tease apart cell type-specific responses, including variation in the functional roles among keratinocytes. Our results suggest a complex interplay of genes and cell types associated with sea lice response in both Atlantic salmon and coho salmon. The susceptibility of Atlantic salmon to sea lice infection despite clear activation of the complement, innate, and adaptive immune systems confirms the insufficiency of this species immune response to effectively repel sea lice. Coho salmon, on the other hand, demonstrate multiple strategies in response to sea lice but keratinocytes seem to be key to the epithelial hyperplasia underlying coho salmon sea lice resistance.

The candidate genes we identified underlying coho salmon's resistance and Atlantic salmon's susceptibility hold significant promise for improving sea lice resistance in Atlantic salmon. Given that transcriptional abundance may not correlate with protein abundance, future proteomic investigation of these candidates would be useful to confirm their association with sea lice resistance.

Additionally, spatial transcriptomics or fluorescence in situ hybridization could be helpful to confirm the localized expression of these candidate genes at the site of sea louse attachment [172].

Gene editing of these candidates could also confirm their functional relevance to sea lice resistance and could also be exploited to confer greater resistance in edited Atlantic salmon. Knocking out genes in Atlantic salmon that we identified as upregulated during lice infestation and potentially linked to immunodeficiency and sea lice immunomodulation (e.g. by inducing a nonsense mutation with CRISPR-Cas9 editing) holds the potential to significantly enhance Atlantic salmon's resistance to sea lice. Furthermore, editing of the promoter region to increase transcription of those genes associated with a dampened immune response in Atlantic salmon or those associated with epithelial hyperplasia in coho salmon could also effectively strengthen lice resistance in Atlantic salmon. Gene editing provides a potential means for proving the function of these genes and their effectiveness in providing host resistance to sea lice [17]; however, uncertainty exists about the public acceptance of the use of this technology for the commercial production of food fish in some jurisdictions, and the risk and benefits of taking any gene editing approach for seafood production should be assessed on a case-by-case basis [173]. Our study has provided important new insights into the cellular and genetic mechanisms that result in an effective host immune response against sea lice. Further investigation is needed to develop effective ways of applying this knowledge, whether through gene editing or other means, to mitigate the fish welfare, economic and ecological toll of sea lice infestations on the Atlantic salmon aquaculture industry.

Methods

Experimental design

Atlantic salmon eggs of the commercial strain of Benchmark Genetics were donated by Benchmark Genetics Iceland. These eggs were from families with less than average estimated breeding values for sea lice resistance (as assessed by Benchmark Genetics based on internally conducted sea lice challenge studies) to represent Atlantic salmon with levels of resistance to lice similar to those of natural populations (i.e. prior to selection for sea lice resistance within the breeding program). Coho salmon (1–2 g) were provided by the Quinsam River Hatchery, Quinsam River, British Columbia, Canada. Wild caught coho were stripped, eggs and milt fertilized, and both species were shipped and reared in a Recirculating Aquaculture System at the Center for Aquaculture Technologies (Prince Edward Island, Canada) in freshwater until post-smolt stage (approximately 15 g), after which fish

were gradually transferred to saltwater and reared to a target weight of approximately 25 g. During the experiment, fish were kept in 135 L tanks at approximately 12 °C. Triplicate tanks of each species were treated with locally sourced ($n=49$ /fish [150]) *Lepeophtheirus salmonis* copepodids, maintained for 60 h and sampled every 12 h. Untreated control fish were maintained in parallel tanks and sampled at 36 h into the experiment. Fish were sedated before sampling with tricaine methanesulfonate (100 mg L^{-1}), and then subjected to a lethal blow to the head. Tissue samples (skin and pelvic fin), from louse attachment sites for treated fish, were collected and immediately frozen in dry ice.

Library preparation and sequencing

Nuclei were isolated from one skin and one fin sample from each of the 5 treatment time points (12 h, 24 h, 36 h, 48 h, and 60 h post exposure) as well as the control for each species ($N=24$ tissue samples total) using a custom protocol optimized for salmon epidermis [174]. In brief, approximately 45 mg tissue samples were cut with scissors in 1 mL of TST buffer for 10 min on ice before being filtered through a 40- μm Falcon™ cell strainer (Thermo Fisher Scientific, catalog no. 08-771-2). A further 1 mL of TST and 3 mL of 1X PBS+BSA buffer were added to each sample before centrifuging at 4 °C for 5 min at 500 g. Samples were resuspended in 1 mL 1X ST buffer filtered again through a 40- μm cell strainer, stained with Hoechst 33342 Solution (Thermo Fisher Scientific, catalog no. 62249) and then nuclei integrity was visually assessed using a fluorescent microscope. A disposable flow haemocytometer (C-Chip Neubauer Improved (100 μm depth), NanoEnTek, catalog no. DHC-N01) was then used to estimate nuclei counts.

Samples were processed with Chromium Next GEM Single Cell 3' Reagent Kits v3.1 (Dual Index) (10X Genomics) using the protocol outlined in the user guide (CG000315 Rev C). Samples were diluted with nuclease-free water to a target concentration that would recover approximately 7000 nuclei in the final library. Samples were then loaded on the Chromium Controller for nuclei droplet formation. After subsequent nuclei and UMI (unique molecular identifier) barcoding and reverse transcription, resulting cDNA was then amplified, fragmented, and indexed with Truseq adapters and Illumina sample indexes. Sequencing was performed on a NovaSeq 6000 platform (Illumina) by Azenta or by Novogene UK Ltd for approximately 220 million paired end 150 bp reads per sample.

Genome indexing and read alignment with STAR

Genome indexing and library mapping was performed with STAR (version 2.7.10a [175, 176]). We appended

the mitochondrial genome from the ENSEMBL V2 Atlantic salmon genome (*Salmo salar*.ICSASG_v2.dna_rm.toplevel.fa.gz, v2, release 105, masked genome, assembly ID: GCA_000233375.4) to the ENSEMBL V3 Atlantic salmon genome (*Salmo salar*.Ssal_v3.1.dna_rm.toplevel.fa.gz, v3.1, release 106, masked genome, assembly ID: GCA_905237065.2) for both the .gff and .fna files prior to indexing. For coho salmon, we appended this species' mitochondrial genome (version NC_009263.1, NCBI) to the ENSEMBL V2 coho salmon genome (*Oncorhynchus kisutch*.Okis_V2.dna_rm.toplevel.fa.gz, v2, release 106, masked genome, assembly ID: GCA_002021735.2) for both the .gff and .fna files prior to indexing. Prior to this concatenation, the coho salmon mitochondrial genome .gff file was manually edited to convert "CDS" annotations to "exon" annotations (consistent with the Atlantic salmon mitochondrial genome .gff file) as STAR assigns transcripts to "exon" annotations in the .gff file. Gffread (v0.10.1) was used to convert .gff to .gtf files [177]. Both genomes were indexed using STAR (--run-Mode genomeGenerate). Each library was then mapped against its corresponding genome with the 10X V3 cell barcode whitelist (3M-february-2018.txt) and using standard parameters for single cell libraries (--soloMultiMappers Unique --soloType CB_UMI_Simple --soloUMIlen 12 --soloCBwhitelist 3M-february-2018.txt --soloFeatures GeneFull --clipAdapterType CellRanger4 --outFilterScoreMin 30 --soloCBmatchWltype 1MM_multi_Nbase_pseudocounts --soloUMIfiltering MultiGeneUMI_CR --soloUMIIdedup 1MM_CR --read-FilesCommand zcat --outSAMtype BAM Unsorted). The raw (unfiltered) files (*genes.tsv*, *barcodes.tsv*, and *matrix.mtx*) generated for each sample were then used for downstream analysis. On average, there were 300 million reads per sample with 94% of reads with valid barcodes and a 62% saturation (for more details see Additional file 1: Fig. S38, Tables S1, S2).

Quality control, clustering, and integration

Seurat objects were then generated in an R (v4.2.0) [178] environment using Seurat (v4.1.1 [179]). We first created individual Seurat objects for each library after removing nuclei with less than 200 features and features occurring in fewer than three nuclei. One Atlantic salmon sample (Atlantic_12h_fin) retained only 60 nuclei after this initial filtration and was therefore discarded from downstream analysis (Additional file 1: Table S3). We then merged samples by species into a single Seurat object. MtDNA features generally accounted for less than 10% of UMIs per cell across samples; however, much higher percentages (>50%) were observed in a minority of cells. Given high mtDNA feature expression can indicate poor quality cells, therefore, nuclei where mtDNA features accounted

for 10% or more of their total UMIs were removed from subsequent analysis (Additional file 1: Table S3, Fig. S39) and then all mtDNA features were removed from the Seurat objects (leaving 48,608 and 39,312 features remaining for Atlantic salmon and coho salmon, respectively). After sub-setting the Seurat object into individual samples, upper and lower thresholds for UMI and feature counts per nuclei were then applied individually to each sample based on knee plot visualization. For all Atlantic salmon samples, only nuclei with more than 500 UMIs but less than 6000 UMIs and more than 500 features and less than 3500 features were retained (Additional file 1: Fig. S40). For coho salmon samples, a lower UMI and feature count limit of 300, 500, or 750 was applied to each sample; an upper UMI limit of 2000 or 6000 was applied while an upper feature limit of 1500 or 3500 was applied (Additional file 1: Fig. S41). A single Atlantic salmon sample (Atlantic_24h_fin) retained only 338 nuclei after this initial filtration and was therefore discarded from downstream analysis (Additional file 1: Table S3).

Samples were then merged again into a single Seurat object by species before splitting samples again into individual sample datasets. This was done to ensure that the same features were considered across samples. Counts were then normalized for each sample using the “NormalizeData” function prior to calculating cell cycle scores using the “CellCycleScoring” function (see Tables S8, S9 for list of genes used). The “v2” SCT (SCTransform) version with the glmGamPoi method (v 1.8.0 [180]) was used to normalize RNA counts for each sample, regressing out scores for the S and G2M cell cycle stages. Linear dimension reduction was conducted for each sample using the “RunPCA” function with 50 PCs (principal components). After consulting Elbowplots for each sample, a UMAP (Uniform Manifold Approximation and Projection) using 20 PCs was run for each sample and the “FindNeighbours” function was applied using 20 PCs, before using the “FindClusters” function with a resolution of 0.2. DoubletFinder (v 2.0.3 [181]) was then applied independently to each sample selecting pK values with the highest associated BCmvn value. We assumed a 4% doublet formation rate (based on the Chromium instrument specifications) and adjusted for homotypic doublets (see Additional file 1: Table S3 for remaining cells per sample after doublet removal).

Samples were integrated by species using 5000 features and anchors that were identified with the “rpca” (reciprocal principal component analysis) reduction method and the “FindIntegrationAnchors” function. A PCA (principal component analysis) was rerun on the integrated dataset using 50 PCs, and 30 PCs were used for subsequent UMAP generation and clustering with a resolution of 0.2 (Additional file 1: Figs. S42a, S43a). Markers for

each cluster were assessed using the logistic regression method and the “FindAllMarkers” function on the “SCT” assay and “data” slot, using sample ID as a latent variable to help reduce batch effects among samples. We used a pseudocount of 0.001, set a p value threshold of 0.01, and only considered genes that were upregulated, expressed in at least 25% of all nuclei (in either of the compared groups), and demonstrated a threshold of 0.25 X difference (log-scale) between the two compared groups.

Two clusters (0 and 4) were removed from the Atlantic salmon dataset due to low average feature/UMI counts (Additional file 1: Fig. S42c, d). Many of the marker genes for cluster 0 were ribosomal genes, suggesting poor quality nuclei (Additional file 1: Fig. S44). Cluster 4 was also found almost exclusively in a single sample (Atlantic_Control_skin), again suggesting it was poor quality (Additional file 1: Fig. S42b). Similarly, cluster 1 from the coho salmon dataset was removed for having low average feature/UMI counts and because many of its markers were ribosomal genes (Additional file 1: Figs. S43c, d, S45). The SCTransformation was then redone for each sample based on the RNA assay as described above, and integration of samples for each species was conducted as described above using 30 PCs for UMAP generation and a resolution of 0.2 for clustering for Atlantic salmon and 20 PCs for UMAP generation and a resolution of 0.2 for clustering for coho salmon. An additional cluster (11) was subsequently removed from the coho salmon dataset for having many ribosomal marker genes (Additional file 1: Figs. S46, S47). The SCTransformation of each sample and integration of samples was again redone for the coho salmon dataset after removing this cluster, again using 20 PCs for UMAP generation and a resolution of 0.2 for clustering. After all filtering, the mean number of UMIs per sample varied from 1056 (Atlantic_48h_fin) to 2824 (Atlantic_60h_fin) in Atlantic salmon and from 518 (Coho_12h_skin) to 2470 (Coho_12h_fin) in coho salmon. The median numbers of UMIs per sample varied from 845.5 (Atlantic_48h_fin) to 2673 (Atlantic_60h_fin) in Atlantic salmon and from 450 (Coho_12h_skin) to 2048 (Coho_12h_fin) in coho salmon. The mean number of features per sample varied from 797 (Atlantic_48h_fin) to 1635 (Atlantic_60h_fin) in Atlantic salmon and from 440 (Coho_12h_skin) to 1562 (Coho_12h_fin) in coho salmon. The median numbers of features per sample varied from 678 (Atlantic_48h_fin) to 1641 (Atlantic_60h_fin) in Atlantic salmon and from 391.5 (Coho_12h_skin) to 1451 (Coho_60h_fin) in coho salmon (Additional file 1: Fig. S48).

Sub-clustering

Clusters identified as immune cells based on the expression (Additional file 1: Fig. S8) of *cd45* (*ptprc*) (a marker

gene for immune cells [97]) were then considered separately for each species to investigate for the presence of additional immune cell types. For immune cells identified within Atlantic salmon samples, a PCA was rerun on the integrated assay using 10 PCs, and UMAP generation and clustering were conducted using 9 PCs and a resolution of 0.3, respectively. For coho salmon immune cells, a PCA was rerun on the integrated dataset using 20 PCs, UMAP was generated using 15 PCs, and clustering was conducted using a resolution of 0.4. Marker genes comparing each immune cell cluster with all other immune cells were then identified using the same marker gene detection method described above using the “FindAllMarkers” function but UMI counts were not re-corrected based on the sub-setted datasets (`recorrect_umi=FALSE`). Marker genes were investigated and visualized to assess cell type. All clusters identified as macrophages were grouped together as were all clusters identified as T cells (see “Results”).

Within a single cluster of the coho salmon dataset (cluster 12), we observed expression of the *ltk* gene (a marker of neural crest cells in Atlantic salmon, see “Results”) in a small subset of cells within this cluster while other cells within this cluster demonstrated expression of *casq1b* (a marker of muscle cells in Atlantic salmon, see “Results”) (Additional file 1: Fig. S49a, b). To investigate the potential for multiple cell types within this cluster, we reran a PCA on cells from this cluster using the integrated assay and 10 PCs, before performing UMAP generation using 3 PCs and clustering with a resolution of 0.02. The resulting UMAP revealed two clusters of cells, one expressing *ltk* and the other expressing *casq1b* (Additional file 1: Fig. S49c–f).

These detected subclusters were then incorporated into the larger dataset for each species including all cell types. The mean number of UMIs per cell type varied from 895 (red blood cells) to 3215 (monocytes) in Atlantic salmon and from 867 (red blood cells) to 2307 (monocytes) in coho salmon. The median numbers of UMIs per sample varied from 768.5 (red blood cells) to 3127 (monocytes) in Atlantic salmon and from 540 (red blood cells) to 1866 (monocytes) in coho salmon. The mean number of features per sample varied from 657 (red blood cells) to 1868 (monocytes) in Atlantic salmon and from 509 (red blood cells) to 1428.5 (monocytes) in coho salmon. The median numbers of features per sample varied from 609 (red blood cells) to 1903 (monocytes) in Atlantic salmon and from 446 (red blood cells) to 1294 (intermediate keratinocytes) in coho salmon (Additional file 1: Fig. S50).

Marker genes were then assessed for all newly identified immune cell types using the “FindAllMarkers” function (as described above) in the context of all other cell

types. The top markers based on the average log twofold change were then considered for each cluster to assess cell type identity. Gene annotations from the ENSEMBL genome were supplemented with EntrezID (NCBI [182]) and UniProt [183] annotations based on querying BioMart (v 2.50.3 [184]).

Differential gene expression detection

We next identified genes which were differentially expressed between the control samples and each of the infection time points (12 h, 24 h, 36 h, 48 h, 60 h post infection) for both species and all cell types using the “FindMarkers” function and the default Wilcox method. We used the SCT assay and “data” slot, imposed a minimum fractional threshold (proportion of cells in either considered group that had to express the gene) of 0.1, set a minimum threshold *p* value of 0.01, and used a threshold of 0.25 X difference (log-scale) between the two compared groups. We excluded results from cell types that had fewer than 50 nuclei in the control samples and comparisons where the treatment time point had fewer than 50 nuclei. Genes were considered differentially expressed if their adjusted *p* value < 0.001. Enriched GO biological processes for differentially expressed genes detected for each cell type for each species were identified using ShinyGO (v 0.80 [185]). We used default parameters and limited the gene universe to all features in the RNA assay for each species (*N*=48,608, *N*=39,312 genes for Atlantic salmon and coho salmon, respectively). GO terms were considered significantly enriched if the FDR (false discovery rate)-adjusted *p* value < 0.001.

Integration of samples across species

We then directly compared Atlantic salmon and coho salmon samples using 6494 genes identified using Orthofinder v2.5.4 [186] as 1:1 orthologs between the two species. The transcriptomes of the Atlantic salmon and coho salmon ENSEMBL genomes used as reference for the snRNAseq analyses were used (*Salmo salar*. *Ssal_v3.1.cdna.all.fa* and *Oncorhynchus kisutch*. *Okis_V2.cdna.all.fa*). A single isoform per gene was retained using a custom python script that selects the longest transcript for each gene, and Orthofinder was run using default parameters. The orthogroups with one gene per species were considered 1:1 orthologs between Atlantic salmon and coho salmon.

Atlantic salmon and coho salmon samples were re-processed using the same quality control methods as described above, but features were winnowed down to this set of 1:1 orthologous genes just prior to the SCTransformation of individual samples. Samples from both species were then integrated together using 2000 features using anchors identified with the “rpca”

reduction method with the “FindIntegrationAnchors” function. A PCA was run on the integrated dataset using 50 PCs with clustering and a UMAP was generated using 20 PCs and a resolution of 0.2. Markers were then detected for each cluster and species using the “FindAllMarkers” function as described above. The distribution of features and UMIs as well as the top markers based on the average log twofold change were then considered for each cluster. A single cluster (cluster 0) was removed due to a lack of defining marker genes (Additional file 1: Figs. S51, S52), following reclustering as above a second cluster (cluster 1) was again removed due to a lack of defining marker genes (Additional file 1: Figs. S53, S54). After removing these clusters, the SCTransformation was redone for each sample based on the RNA assay, and integration of samples for each species was conducted as described above (using 2000 features for integration, 50 PCs for the PCA, 20 PCs and a resolution of 0.2 for clustering and UMAP generation, see Additional file 1: Fig. S55 for distribution of UMIs and features per cell type and cell type counts per sample). Markers were then detected for each cluster using the “FindAllMarkers” function as described above. The top markers based on the average log twofold change were then considered for each cluster to assess cell type identity.

Abbreviations

FDR	False discovery rate
PC	Principal component
PCA	Principal component analysis
rpca	Reciprocal principal component analysis
SCT	SCTransform
snRNAseq	Single-nuclei RNA sequencing
UMAP	Uniform Manifold Approximation and Projection
UMI	Unique molecular identifier

Supplementary Information

The online version contains supplementary material available at <https://doi.org/10.1186/s12915-024-01952-8>.

Additional file 1: Figs. S1–S55 and Tables S1–S9. Figs. S1–S55: Fig. S1

Expression of marker genes within 23 identified cell clusters within Atlantic salmon fin and skin samples. **Fig. S2** Expression of marker genes within 23 identified cell clusters within coho salmon fin and skin samples. **Fig. S3** Violin plots of the expression of marker genes from Fig. 1c for each cell type detected within Atlantic salmon samples split by tissue type. **Fig. S4** Violin plots of the expression of marker genes from Fig. 1d for each cell type detected within coho salmon samples split by tissue type. **Fig. S5** Violin plots of expression levels for the top 20 significant marker genes for the mucous (1) cluster of the coho salmon dataset. **Fig. S6** Violin plots of expression levels for the top 20 significant marker genes for the mucous (2) cluster of the coho salmon dataset. **Fig. S7** Violin plots of expression levels for the top 20 significant marker genes for the undifferentiated cluster of the Atlantic salmon dataset. **Fig. S8** Expression of *CD45* (*ptprc*) in Atlantic salmon (a, b) and coho salmon (c, d). **Fig. S9** Violin plots of expression levels for the top 20 significant marker genes for the T cells (1) cluster of the Atlantic salmon immune cells only data subset. **Fig. S10** Violin plots of expression levels for the top 20 significant marker genes for the T cells (2) cluster of the Atlantic salmon immune cells only data subset. **Fig. S11** Violin plots of expression levels for the top 20 significant marker genes for the T cells (3) cluster of the Atlantic salmon immune cells only

data subset. **Fig. S12** Violin plots of expression levels for the top 20 significant marker genes for the T cells (4) cluster of the Atlantic salmon immune cells only data subset. **Fig. S13** Violin plots of expression levels for the top 20 significant marker genes for the T cells (5) cluster of the Atlantic salmon immune cells only data subset. **Fig. S14** Violin plots of expression levels for the top 20 significant marker genes for neutrophils of the Atlantic salmon immune cells only data subset. **Fig. S15** Violin plots of expression levels for the top 20 significant marker genes for dendritic cells of the Atlantic salmon immune cells only data subset. **Fig. S16** Violin plots of expression levels for the top 20 significant marker genes for neutrophils of the Atlantic salmon immune cells only data subset. **Fig. S17** Violin plots of expression levels for the top 20 significant marker genes for the macrophages (1) cluster of the Atlantic salmon immune cells only data subset. **Fig. S18** Violin plots of expression levels for the top 20 significant marker genes for the macrophages (2) cluster of the Atlantic salmon immune cells only data subset. **Fig. S19** Violin plots of expression levels for the top 20 significant marker genes for the macrophages (3) cluster of the Atlantic salmon immune cells only data subset. **Fig. S20** Violin plots of expression levels for the top 20 significant marker genes for monocytes of the Atlantic salmon immune cells only data subset. **Fig. S21** Violin plots of expression levels for the top 20 significant marker genes for the T cells (1) cluster of the coho salmon immune cells only data subset. **Fig. S22** Violin plots of expression levels for the top 20 significant marker genes for the T cells (2) cluster of the coho salmon immune cells only data subset. **Fig. S23** Violin plots of expression levels for the top 20 significant marker genes for the T cells (3) cluster of the coho salmon immune cells only data subset. **Fig. S24** Violin plots of expression levels for the top 20 significant marker genes for the T cells (4) cluster of the coho salmon immune cells only data subset. **Fig. S25** Violin plots of expression levels for the top 20 significant marker genes for the T cells (5) cluster of the coho salmon immune cells only data subset. **Fig. S26** Violin plots of expression levels for the top 20 significant marker genes for B cells of the coho salmon immune cells only data subset. **Fig. S27** Violin plots of expression levels for the top 20 significant marker genes for dendritic cells of the coho salmon immune cells only data subset. **Fig. S28** Violin plots of expression levels for the top 20 significant marker genes for neutrophils of the coho salmon immune cells only data subset. **Fig. S29** Violin plots of expression levels for the top 20 significant marker genes for the macrophages (1) cluster of the coho salmon immune cells only data subset. **Fig. S30** Violin plots of expression levels for the top 20 significant marker genes for the macrophages (2) cluster of the coho salmon immune cells only data subset. **Fig. S31** Violin plots of expression levels for the top 20 significant marker genes for monocytes of the coho salmon immune cells only data subset. **Fig. S32** Expression of *CD4* and *CD8* paralogs in the immune cell subclusters identified within a) Atlantic salmon and b) coho salmon. **Fig. S33** Number of genes detected as differentially expressed between the control samples and each of the infected time points for each cell type for a) Atlantic salmon and b) coho salmon. **Fig. S34** Number of times each gene was detected as differentially expressed (1–5 time points) between any of the treatment time points and the control sample for a given cell type detected within the Atlantic salmon samples. **Fig. S35** Number of times each gene was detected as differentially expressed (1–5 time points) between any of the treatment time points and the control sample for a given cell type detected within the coho salmon samples. **Fig. S36** Significantly enriched biological GO terms for each Atlantic salmon cell type based on the significantly differentially expressed genes detected between the control samples and any of the five treatment time points. **Fig. S37** Significantly enriched biological GO terms for each coho salmon cell type based on the significantly differentially expressed genes detected between the control samples and any of the five treatment time points. **Fig. S38** Summary statistics for all Atlantic and coho salmon libraries. **Fig. S39** Percent of UMIs identified as mtDNA features for a) Atlantic salmon and b) coho salmon samples, with the 10% maximum threshold used for subsequent filtering indicated by a horizontal black line. **Fig. S40** UMI and feature counts per cell barcode and feature counts vs. UMI counts for each Atlantic salmon sample. **Fig. S41** UMI and feature counts per cell barcode and feature counts vs. UMI counts for each coho salmon sample. **Fig. S42** Cell clusters after initial integration of Atlantic salmon samples: a) UMAP, b) number of cells per cluster per sample, c) violin plot of the distribution of feature counts per cluster, d) violin plot of the distribution of UMI counts

per cluster. **Fig. S43** Cell clusters after initial integration of coho salmon samples: a) UMAP, b) number of cells per cluster per sample, c) violin plot of the distribution of feature counts per cluster, d) violin plot of the distribution of UMI counts per cluster. **Fig. S44** Violin plots of expression levels for the top 20 significant marker genes for cluster 0 after the initial integration of Atlantic salmon samples. **Fig. S45** Violin plots of expression levels for the top 20 significant marker genes for cluster 1 after the initial integration of coho salmon samples. **Fig. S46** Cell clusters after removing one cluster (cluster 1 from Fig. S43) and re-integrating/clustering coho salmon samples: a) UMAP, b) number of cells per cluster per sample, c) violin plot of the distribution of feature counts per cluster, d) violin plot of the distribution of UMI counts per cluster. **Fig. S47** Violin plots of expression levels for the top 20 significant marker genes for cluster 11 after removing one cluster (cluster 1 from Fig. S43) and re-integrating/clustering coho salmon samples. **Fig. S48** Distribution of UMIs and features for Atlantic salmon (a, b) and coho salmon (c, d) samples. **Fig. S49** Subclustering of cluster 12 within coho salmon. Feature plots indicate expression of *ltk* (a) and *casq1b* (b) in different cells within cluster 12. Reclustering those cells within cluster 12 using 3 PCs and a resolution of 0.02 revealed two clusters as visualized in a UMAP (c). One cluster expressed *casq1b*, the other expressed *ltk* as shown in a dot plot (d) and feature plots (e, f). **Fig. S50** Distribution of UMIs and features for each cluster identified in Atlantic salmon (a, b) and coho salmon (c, d). **Fig. S51** Cell clusters after initial integration of Atlantic and coho salmon samples: a) UMAP, b) number of cells per cluster per sample, c) violin plot of the distribution of feature counts per cluster, d) violin plot of the distribution of UMI counts per cluster. **Fig. S52** Violin plots of expression levels for the 9 significant marker genes for cluster 0 of the dataset integrating both Atlantic salmon and coho salmon samples. **Fig. S53** Cell clusters after removing one cluster (cluster 0 from Fig. S51) and re-integrating/clustering: a) UMAP, b) number of cells per cluster per sample, c) violin plot of the distribution of feature counts per cluster, d) violin plot of the distribution of UMI counts per cluster. **Fig. S54** Violin plots of expression levels for the 7 significant marker genes for cluster 1 of the dataset integrating both Atlantic and coho samples (for UMAP see Fig. S53). **Fig. S55** Cell clusters after removing one cluster (cluster 1 from Fig. S53) and re-integrating/clustering: a) violin plot of the distribution of feature counts per cluster, b) violin plot of the distribution of UMI counts per cluster, c) number of cells per cluster per sample. **Tables S1–S9: Table S1** Summary statistics for STAR outputs for each Atlantic salmon sample. **Table S2** Summary statistics for STAR outputs for each coho salmon sample. **Table S3** Number of nuclei detected per sample after several filtering stages. **Table S4** Number of cells per cell type in each Atlantic salmon sample. **Table S5** Number of cells per cell type in each coho salmon sample. **Table S6** Number of cells per cluster and sampling time point after reclustering only the immune cells within the Atlantic salmon samples. **Table S7** Number of cells per cluster after reclustering only the immune cells within the coho salmon samples. **Table S8** Genes used for cell cycle scoring for Atlantic salmon. **Table S9** Genes used for cell cycle scoring for coho salmon.

Additional file 2: Six excel sheets. AS_MARKERS: marker genes detected for each cell type in the Atlantic salmon dataset. **CO_MARKERS:** marker genes detected for each cell type in the coho salmon dataset. **ASCO_MARKERS:** marker genes detected for each cell type in the dataset integrating both Atlantic salmon and coho salmon samples. **AS_IMMUNE_ONLY_MARKERS:** marker genes detected for each immune cell subcluster in the Atlantic salmon dataset. **CO_IMMUNE_ONLY_MARKERS:** marker genes detected for each immune cell subcluster in the coho salmon dataset. **AS_DE:** differentially expressed genes between control and treatment groups for each cell type and treatment time point in Atlantic salmon. **CO_DE:** differentially expressed genes between control and treatment groups for each cell type and treatment time point in coho salmon.

Acknowledgements

Our thanks go to two anonymous reviewers and our editor for their helpful comments on our manuscript. We gratefully acknowledge Paige Ackerman, Edward Walls, Sherri Higgins, and Cindy Ederis for contributing coho salmon

from Quinsam River Hatchery as well as Ólafur H. Kristjánsson of StofnFiskur, Benchmark Genetics in Iceland and Morten Rye of Benchmark Genetics in Norway for contributing Atlantic salmon eggs. Our thanks go to Dr Mark Polinski and Russell Anderson from FAS delivery for ensuring the safe and efficient transfer of animals and Dr Mark Braceland and Dr Hiatham Mohammed from CATC, as well as Dylan Michaud for ensuring the welfare of animals throughout the experiment. Thanks to Marlene Atlas for assistance with proofreading.

Authors' contributions

MDF, SJM, JEB, MDF, RDH, NR, and DR created the experimental design. MDF, RRD, and DR conducted the experiment and collected tissue samples. RRD led the lab work with assistance from SJS, PRV, and OG. SJS led the data analysis, interpretation, and figure generation, with assistance from DR. SJS led the writing in consultation with DR and with assistance from RRD, SJM, JEB, PRV, MDF, LS, RDH, and NR. All authors read and approved the final manuscript.

Funding

This work was supported by FHF grant 901631 ("CrispResist"), BBSRC grants BB/V009818-1 and BB/V009990/1 ("GenoLice"), and BBSRC Institute Strategic Grants to the Roslin Institute (BBS/E/D/20002172, BBS/E/D/30002275, BBS/E/D/10002070, and BBS/E/RL/230002A). SJS gratefully acknowledges funding from an NSERC PDF award.

Availability of data and materials

Raw sequencing data and STAR output files (barcode, feature, and matrix files) for all samples used in this study are available on NCBI's Gene Expression Omnibus (series: GSE269132, samples: GSM8306834–GSM8306857 [187]). Scripts used to analyse and visualize data are available at https://github.com/SarahSalisbury/Atlantic_Salmon_vs_Coho_Salmon_Lice_Response_snRNA_seq.

Declarations

Ethics approval and consent to participate

CATC and UPEI Animal Care Committees (AUP 21–008) approved all fish handling procedures, which were conducted in accordance with the Canadian Council for Animal Care regulations (<http://www.ccaac.ca/>) and ARRIVE guidelines.

Consent for publication

Not applicable.

Competing interests

The authors declare that they have no competing interests.

Author details

¹The Roslin Institute and Royal (Dick) School of Veterinary Studies, University of Edinburgh, Edinburgh, UK. ²Institute of Aquaculture, University of Stirling, Stirling, UK. ³Department of Genetics, University of Santiago de Compostela, Santiago de Compostela, Spain. ⁴Atlantic Veterinary College, University of Prince Edward Island, Charlottetown, Canada. ⁵Nofima AS, Tromsø, Norway. ⁶Benchmark Genetics, 1 Pioneer Building Milton Bridge, Edinburgh Technopole Penicuik, UK. ⁷Sustainable Aquaculture Laboratory - Temperate and Tropical (SALTT), Deakin University, Melbourne, VIC 3225, Australia.

Received: 15 November 2023 Accepted: 28 June 2024

Published online: 29 July 2024

References

- Brooker AJ, Skern-Mauritzen R, Bron JE. Production, mortality, and infectivity of planktonic larval sea lice, *Lepeophtheirus salmonis* (Krøyer, 1837): current knowledge and implications for epidemiological modelling. *ICES J Mar Sci.* 2018;75(4):1214–34.
- Boxshall GA, Bravo S. On the identity of the common *Caligus* (Copepoda: Siphonostomatoida: Caligidae) from salmonid netpen systems in southern Chile. *Contrib Zool.* 2000;69(1–2):137–46.
- Carvalho LA, Whyte SK, Braden LM, Purcell SL, Manning AJ, Muckle A, Fast MD. Impact of co-infection with *Lepeophtheirus salmonis* and

- Moritella viscosa* on inflammatory and immune responses of Atlantic salmon (*Salmo salar*). J Fish Dis. 2020;43(4):459–73.
4. Abolofia J, Asche F, Wilen JE. The cost of lice: quantifying the impacts of parasitic sea lice on farmed salmon. Mar Res Econ. 2017;32(3):329–49.
 5. Torrissen O, Jones S, Asche F, Guttormsen A, Skilbrei OT, Nilsen F, et al. Salmon lice—impact on wild salmonids and salmon aquaculture. J Fish Dis. 2013;36(3):171–94.
 6. Barrett LT, Oppedal F, Robinson N, Dempster T. Prevention not cure: a review of methods to avoid sea lice infestations in salmon aquaculture. Rev Aquac. 2020;12(4):2527–43.
 7. Burridge L, Weis JS, Cabello F, Pizarro J, Bostick K. Chemical use in salmon aquaculture: a review of current practices and possible environmental effects. Aquaculture. 2010;306(1–4):7–23.
 8. Glover KA, Aasmundstad T, Nilsen F, Storset A, Skaala Ø. Variation of Atlantic salmon families (*Salmo salar* L.) in susceptibility to the sea lice *Lepeophtheirus salmonis* and *Caligus elongatus*. Aquaculture. 2005;245(1–4):19–30.
 9. Gjerde B, Ødegård J, Thorland I. Estimates of genetic variation in the susceptibility of Atlantic salmon (*Salmo salar*) to the salmon louse *Lepeophtheirus salmonis*. Aquaculture. 2011;314(1–4):66–72.
 10. Holborn MK, Rochus CM, Ang KP, Elliott JA, Leadbeater S, Powell F, Boulding EG. Family-based genome wide association analysis for salmon lice (*Lepeophtheirus salmonis*) resistance in North American Atlantic salmon using a 50 K SNP array. Aquaculture. 2019;511:734215.
 11. Tsai HY, Hamilton A, Tinch AE, Guy DR, Bron JE, Taggart JB, et al. Genomic prediction of host resistance to sea lice in farmed Atlantic salmon populations. Genet Sel Evol. 2016;48(1):1–11.
 12. Correa K, Banger A, Figueroa R, Lhorente JP, Yáñez JM. The use of genomic information increases the accuracy of breeding value predictions for sea louse (*Caligus rogercresseyi*) resistance in Atlantic salmon (*Salmo salar*). Genet Sel Evol. 2017;49(1):1–5.
 13. Ødegård J, Medina M, Torgersen JS, Korsvoll SA, Deerenberg R, Yáñez JM, et al. Genetic selection for reduced parasite load in Atlantic salmon: zero-sum game or a tool for group-level protection against sea lice? Aquaculture. 2024;581:740438.
 14. Correa K, Lhorente JP, Bassini L, López ME, Di Genova A, Maass A, et al. Genome wide association study for resistance to *Caligus rogercresseyi* in Atlantic salmon (*Salmo salar* L.) using a 50K SNP genotyping array. Aquaculture. 2017;472:61–5.
 15. Rochus CM, Holborn MK, Ang KP, Elliott JA, Glebe BD, Leadbeater S, et al. Genome-wide association analysis of salmon lice (*Lepeophtheirus salmonis*) resistance in a North American Atlantic salmon population. Aquac Res. 2018;49(3):1329–38.
 16. Robledo D, Gutiérrez AP, Barría A, Lhorente JP, Houston RD, Yáñez JM. Discovery and functional annotation of quantitative trait loci affecting resistance to sea lice in Atlantic salmon. Front Genet. 2019;10:56.
 17. Robinson NA, Robledo D, Sveen L, Ruiz Daniels R, Krasnov A, Coates A, et al. Applying genetic technologies to combat infectious diseases in aquaculture. Rev Aquac. 2023;15(2):491–535.
 18. Johnson SC, Albright LJ. Comparative susceptibility and histopathology of the response of naive Atlantic, chinook and coho salmon to experimental infection with *Lepeophtheirus salmonis* (Copepoda: Caligidae). Dis Aquat Organ. 1992;14(3):179–93.
 19. Fast MD. Fish immune responses to parasitic copepod (namely sea lice) infection. Dev Comp Immunol. 2014;43(2):300–12.
 20. Braden LM, Michaud D, Groman D, Byrne P, Hori TS, Fast MD. Rejection of *Lepeophtheirus salmonis* driven in part by chitin sensing is not impacted by seawater acclimatization in Coho salmon (*Oncorhynchus kisutch*). Sci Rep. 2023;13(1):1–19.
 21. Fast MD, Sims DE, Burka JF, Mustafa A, Ross NW. Skin morphology and humoral non-specific defence parameters of mucus and plasma in rainbow trout, coho and Atlantic salmon. Comp Biochem Physiol A Mol Integr Physiol. 2002;132(3):645–57.
 22. Johnson SC, Fast MD. Interactions between sea lice and their hosts. In: Wiegertjes GF, Flik G, editors. Host-parasite interactions. Abingdon, UK: Taylor & Francis; 2004. p. 131–59.
 23. Valenzuela-Muñoz V, Bolaña S, Gallardo-Escárate C. Comparative immunity of *Salmo salar* and *Oncorhynchus kisutch* during infestation with the sea louse *Caligus rogercresseyi*: an enrichment transcriptome analysis. Fish Shellfish Immunol. 2016;59:276–87.
 24. Fast MD, Braden LM. Salmon-lice interaction and immunological consequences for the host. In: Treasurer J, Bricknell IR, Bron JE, editors. Sea lice biology and control. Essex UK: 5M Books Ltd; 2022. p. 272–93.
 25. Braden LM, Koop BF, Jones SR. Signatures of resistance to *Lepeophtheirus salmonis* include a TH2-type response at the louse-salmon interface. Dev Comp Immunol. 2015;48(1):178–91.
 26. Valenzuela-Muñoz V, Bolaña S, Gallardo-Escárate C. Uncovering iron regulation with species-specific transcriptome patterns in Atlantic salmon and coho salmon during a *Caligus rogercresseyi* infestation. J Fish Dis. 2017;40(9):1169–84.
 27. Murdoch CC, Skaar EP. Nutritional immunity: the battle for nutrient metals at the host–pathogen interface. Nat Rev Microbiol. 2022;20(11):657–70.
 28. Sveen LR, Robinson N, Krasnov A, Ruiz Daniels R, Vaadal M, Karlsen C, et al. Transcriptomic landscape of Atlantic salmon (*Salmo salar* L.) skin. G3. 2023;13(11):jkad215.
 29. Hawkes JW. The structure of fish skin: I. General organization Cell Tissue Res. 1974;149(2):147–58.
 30. Quilhac A, Sire JY. Spreading, proliferation, and differentiation of the epidermis after wounding a cichlid fish, *Hemichromis bimaculatus*. Anat Rec. 1999;254(3):435–51.
 31. Sveen L, Karlsen C, Ytteborg E. Mechanical induced wounds in fish—a review on models and healing mechanisms. Rev Aquac. 2020;12(4):2446–65.
 32. Elliott DG. THE SKIN| Functional morphology of the integumentary system in fishes. In: Farrell AP. Encyclopedia of fish physiology. Academic Press. 2011. p. 476–88.
 33. Elliott DG. Integumentary system. In: The laboratory fish. Academic Press; 2000. p. 271–306.
 34. Sehring IM, Weidinger G. Recent advancements in understanding fin regeneration in zebrafish. Wiley Interdiscip Rev Dev Biol. 2020;9(1):e367.
 35. Rasmussen JP, Vo NT, Sagasti A. Fish scales dictate the pattern of adult skin innervation and vascularization. Dev Cell. 2018;46(3):344–59.
 36. Esteban MÁ, Cerezuela R. Fish mucosal immunity: skin. In: Beck BH, Peatman E. Mucosal health in aquaculture. Academic Press. 2015. p. 67–92.
 37. Chen G, Ning B, Shi T. Single-cell RNA-seq technologies and related computational data analysis. Front Genet. 2019;10:317.
 38. Kolodziejczyk AA, Kim JK, Svensson V, Marioni JC, Teichmann SA. The technology and biology of single-cell RNA sequencing. Mol Cell. 2015;58(4):610–20.
 39. Sun S, Liu Z, Jiang Q, Zou Y. Embryonic expression patterns of *TBC1D10* subfamily genes in zebrafish. Gene Expr Patterns. 2022;43:119226.
 40. Carmona SJ, Teichmann SA, Ferreira L, Macaulay IC, Stubbington MJ, Cvejic A, et al. Single-cell transcriptome analysis of fish immune cells provides insight into the evolution of vertebrate immune cell types. Genome Res. 2017;27(3):451–61.
 41. Raab M, Wang H, Lu Y, Smith X, Wu Z, Strebhardt K, et al. T cell receptor “inside-out” pathway via signaling module *SKAP1*-RapL regulates T cell motility and interactions in lymph nodes. Immunity. 2010;32(4):541–56.
 42. Mason DY, Cordell J, Brown M, Pallesen G, Ralfkiaer E, Rothbard J, Crumpton M, Gatter KC. Detection of T cells in paraffin wax embedded tissue using antibodies against a peptide sequence from the *CD3* antigen. J Clin Pathol. 1989;42(11):194–200.
 43. Lang G, Wotton D, Owen MJ, Sewell WA, Brown MH, Mason DY, et al. The structure of the human *CD2* gene and its expression in transgenic mice. EMBO J. 1988;7(6):1675–82.
 44. Nechanitzky R, Akbas D, Scherer S, Györy I, Hoyle T, Ramamoorthy S, et al. Transcription factor *EBF1* is essential for the maintenance of B cell identity and prevention of alternative fates in committed cells. Nat Immunol. 2013;14(8):867–75.
 45. Borggrete T, Keshavarzi S, Gross B, Wabl M, Jessberger R. Impaired *IgE* response in *SWAP-70*-deficient mice. Eur J Immunol. 2001;31(8):2467–75.
 46. Liu X, Li YS, Shinton SA, Rhodes J, Tang L, Feng H, et al. Zebrafish B cell development without a pre-B cell stage, revealed by *CD79* fluorescence reporter transgenes. J Immunol. 2017;199(5):1706–15.
 47. Karsunky H, Merad M, Cozzio A, Weissman IL, Manz MG. *Flt3* ligand regulates dendritic cell development from *Flt3+* lymphoid and myeloid-committed progenitors to *Flt3+* dendritic cells in vivo. J Exp Med. 2003;198(2):305–13.

48. Marafioti T, Paterson JC, Ballabio E, Reichard KK, Tedoldi S, Hollowood K, et al. Novel markers of normal and neoplastic human plasmacytoid dendritic cells. *Blood*. 2008;111(7):3778–92.
49. Liu F, Wu HY, Wesselschmidt R, Kornaga T, Link DC. Impaired production and increased apoptosis of neutrophils in granulocyte colony-stimulating factor receptor-deficient mice. *Immunity*. 1996;5(5):491–501.
50. Taylor RS, Ruiz Daniels R, Dobie R, Naseer S, Clark TC, Henderson NC, et al. Single cell transcriptomics of Atlantic salmon (*Salmo salar* L.) liver reveals cellular heterogeneity and immunological responses to challenge by *Aeromonas salmonicida*. *Front Immunol*. 2022;13:984799.
51. Sharma A, Rijavec M, Tomar S, Yamani A, Ganesan V, Kremplis J, et al. Acute systemic myeloid inflammatory and stress response in severe food allergic reactions. *Clin Exp Allergy*. 2023;53(5):536–49.
52. Ito D, Kumanogoh A. The role of *Sema4A* in angiogenesis, immune responses, carcinogenesis, and retinal systems. *Cell Adh Migr*. 2016;10(6):692–9.
53. Sehgal A, Donaldson DS, Pridans C, Sauter KA, Hume DA, Mabbott NA. The role of *CSF1R*-dependent macrophages in control of the intestinal stem-cell niche. *Nat Commun*. 2018;9(1):1272.
54. Farnsworth DR, Saunders LM, Miller AC. A single-cell transcriptome atlas for zebrafish development. *Dev Biol*. 2020;459(2):100–8.
55. Liuzzo JP, Petanceska SS, Moscatelli D, Devi LA. Inflammatory mediators regulate cathepsin S in macrophages and microglia: a role in attenuating heparan sulfate interactions. *Mol Med*. 1999;5:320–33.
56. Anbazhagan K, Duroux-Richard I, Jorgensen C, Apparailly F. Transcriptomic network support distinct roles of classical and non-classical monocytes in human. *Int Rev Immunol*. 2014;33(6):470–89.
57. Subkhankulova T, Camargo Sosa K, Uroshlev LA, Nikaido M, Shriever N, Kasianov AS, et al. Zebrafish pigment cells develop directly from persistent highly multipotent progenitors. *Nat Commun*. 2023;14(1):1258.
58. Ruhrberg C, Hajibagheri MN, Parry DA, Watt FM. Periplakin, a novel component of cornified envelopes and desmosomes that belongs to the plakin family and forms complexes with envoplakin. *J Cell Biol*. 1997;139(7):1835–49.
59. Berdyshev E, Goleva E, Bronova I, Dyjack N, Rios C, Jung J, et al. Lipid abnormalities in atopic skin are driven by type 2 cytokines. *JCI insight*. 2018;3(4):e98006.
60. Perez CJ, Jaubert J, Guénet JL, Barnhart KF, Ross-Inta CM, Quintanilla VC, Aubin I, et al. Two hypomorphic alleles of mouse *Ass1* as a new animal model of citrullinemia type I and other hyperammonemic syndromes. *Am J Pathol*. 2010;177(4):1958–68.
61. Rizzolio F, Bione S, Villa A, Berti E, Cassetti A, Bulfone A, et al. Spatial and temporal expression of *POF1B*, a gene expressed in epithelia. *Gene Expr Patterns*. 2007;7(4):529–34.
62. Malaisse J, Hermant M, Hayez A, Poumay Y, Lambert de Rouvroit C. Meaning of relative gene expression in multilayered cultures of epidermal keratinocytes. *Exp Dermatol*. 2014;23(10):754–6.
63. Brinckmann J, Hunzelmann N, Kahle B, Rohwedel J, Kramer J, Gibson MA, et al. Enhanced fibrillin-2 expression is a general feature of wound healing and sclerosis: potential alteration of cell attachment and storage of *TGF-β*. *Lab Invest*. 2010;90(5):739–52.
64. Koch M, Bohrmann B, Matthison M, Hagios C, Trueb B, Chiquet M. Large and small splice variants of collagen XII: differential expression and ligand binding. *J Cell Biol*. 1995;130(4):1005–14.
65. Usuba R, Pauty J, Soncin F, Matsunaga YT. *EGFL7* regulates sprouting angiogenesis and endothelial integrity in a human blood vessel model. *Biomaterials*. 2019;197:305–16.
66. Ruppert AL, Keshavarz M, Winterberg S, Oberwinkler J, Kummer W, Schütz B. Advillin is a tuft cell marker in the mouse alimentary tract. *J Mol Histol*. 2020;51:421–35.
67. Willms RJ, Jones LO, Hocking JC, Foley E. A cell atlas of microbe-responsive processes in the zebrafish intestine. *Cell Rep*. 2022;38(5):110311.
68. Gerbe F, Sidot E, Smyth DJ, Ohmoto M, Matsumoto I, Dardalhon V, et al. Intestinal epithelial tuft cells initiate type 2 mucosal immunity to helminth parasites. *Nature*. 2016;529(7585):226–30.
69. Middelhoff M, Nienhüser H, Valenti G, Maurer HC, Hayakawa Y, Takahashi R, et al. *Prox1*-positive cells monitor and sustain the murine intestinal epithelial cholinergic niche. *Nat Commun*. 2020;11(1):111.
70. Song Y, Meng Z, Zhang S, Li N, Hu W, Li H. miR-4739/*ITGA10*/*PI3K* signaling regulates differentiation and apoptosis of osteoblast. *Regen Ther*. 2022;21:342–50.
71. Cool S, Jackson R, Pincus P, Dickinson I, Nurcombe V. Fibroblast growth factor receptor 4 (*FGFR4*) expression in newborn murine calvaria and primary osteoblast cultures. *Int J Dev Biol*. 2004;46(4):519–23.
72. Furlan S, Mosole S, Murgia M, Nagaraj N, Argenton F, Volpe P, Nori A. Calsequestrins in skeletal and cardiac muscle from adult *Danio rerio*. *J Muscle Res Cell Motil*. 2016;37:27–39.
73. Yoshimoto Y, Ikemoto-Uezumi M, Hitachi K, Fukada SI, Uezumi A. Methods for accurate assessment of myofiber maturity during skeletal muscle regeneration. *Front Cell Dev Biol*. 2020;8:267.
74. Van der Loop FT, Van Eys GJ, Schaart G, Ramaekers FC. Titin expression as an early indication of heart and skeletal muscle differentiation in vitro. Developmental re-organisation in relation to cytoskeletal constituents. *J Muscle Res Cell Motil*. 1996;17:23–36.
75. Kimura T, Takehana Y, Naruse K. *pnp4a* is the causal gene of the medaka iridophore mutant guanineless. *G3: Genes*. 2017;7(4):1357–63.
76. Santos ME, Braasch I, Boileau N, Meyer BS, Sauteur L, Böhne A, Belting HG, Affolter M, Salzburger W. The evolution of cichlid fish egg-spots is linked with a cis-regulatory change. *Nat Commun*. 2014;5(1):5149.
77. Jang HS, Chen Y, Ge J, Wilkening AN, Hou Y, Lee HJ, Choi YR, Lowdon RF, Xing X, Li D, Kaufman CK. Epigenetic dynamics shaping melanophore and iridophore cell fate in zebrafish. *Genome Biol*. 2021;22:1–18.
78. Yamada S, Sakakibara SI. Expression profile of the *STAND* protein *Nwd1* in the developing and mature mouse central nervous system. *J Comp Neurol*. 2018;526(13):2099–114.
79. Fernandez T, Morgan T, Davis N, Klin A, Morris A, Farhi A, Lifton RP. Disruption of contactin 4 (*CNTN4*) results in developmental delay and other features of 3p deletion syndrome. *Am J Hum Genet*. 2004;74(6):1286–93.
80. Marolilley T, Tsai MH, Mascarenhas R, Diao C, Khanbabaei M, Kaya S, Depienne C, Tarailo-Graovac M, Klein KM. A novel FAME1 repeat configuration in a European family identified using a combined genomics approach. *Epilepsia Open*. 2023;8(2):659–65.
81. Zhou Z, Peng X, Insolera R, Fink DJ, Mata M. Interleukin-10 provides direct trophic support to neurons. *J Neurochem*. 2009;110(5):1617–27.
82. Joseph DB, Henry GH, Malewska A, Reese JC, Mauck RJ, Gahan JC, Hutchinson RC, Malladi VS, Roehrborn CG, Vezina CM, Strand DW. Single-cell analysis of mouse and human prostate reveals novel fibroblasts with specialized distribution and microenvironment interactions. *J Pathol*. 2021;255(2):141–54.
83. He H, Suryawanshi H, Morozov P, Gay-Mimbrera J, Del Duca E, Kim HJ, et al. Single-cell transcriptome analysis of human skin identifies novel fibroblast subpopulation and enrichment of immune subsets in atopic dermatitis. *J Allergy Clin Immunol*. 2020;145(6):1615–28.
84. Song H, Sun W, Ye G, Ding X, Liu Z, Zhang S, et al. Long non-coding RNA expression profile in human gastric cancer and its clinical significances. *J Transl Med*. 2013;11(1):1–10.
85. Park KS, Korfhagen TR, Bruno MD, Kitzmiller JA, Wan H, Wert SE, et al. *SPDEF* regulates goblet cell hyperplasia in the airway epithelium. *J Clin Invest*. 2007;117(4):978–88.
86. Ma J, Rubin BK, Vovnow JA. Mucins, mucus, and goblet cells. *Chest*. 2018;154(1):169–76.
87. Tarr PT, Edwards PA. *ABCG1* and *ABCG4* are coexpressed in neurons and astrocytes of the CNS and regulate cholesterol homeostasis through *SREBP-2*. *J Lipid Res*. 2008;49(1):169–82.
88. Gerrits E, Giannini LA, Brouwer N, Melhem S, Seilhean D, Le Ber I, et al. Neurovascular dysfunction in GRN-associated frontotemporal dementia identified by single-nucleus RNA sequencing of human cerebral cortex. *Nat Neurosci*. 2022;25(8):1034–48.
89. Seale P, Sabourin LA, Girgis-Gabardo A, Mansouri A, Gruss P, Rudnicki MA. *Pax7* is required for the specification of myogenic satellite cells. *Cell*. 2000;102(6):777–86.
90. Kuo DS, Labelle-Dumais C, Gould DB. *COL4A1* and *COL4A2* mutations and disease: insights into pathogenic mechanisms and potential therapeutic targets. *Hum Mol Genet*. 2012;21(R1):R97–110.
91. Vernersson E, Khoo NK, Henriksson ML, Roos G, Palmer RH, Hallberg B. Characterization of the expression of the ALK receptor tyrosine kinase in mice. *Gene Expr Patterns*. 2006;6(5):448–61.
92. Mo ES, Cheng Q, Reshetnyak AV, Schlessinger J, Nicoli S. Alk and Ltk ligands are essential for iridophore development in zebrafish mediated by the receptor tyrosine kinase *Ltk*. *PNAS*. 2017;114(45):12027–32.

93. Sveen LR, Timmerhaus G, Krasnov A, Takle H, Handeland S, Ytteborg E. Wound healing in post-smolt Atlantic salmon (*Salmo salar* L.). *Sci Rep*. 2019;9(11):3565.
94. Uss E, Rowshani AT, Hooibrink B, Lardy NM, van Lier RA, ten Berge JJ. *CD103* is a marker for alloantigen-induced regulatory *CD8+* T cells. *J Immunol*. 2006;177(5):2775–83.
95. Lau SK, Chu PG, Weiss LM. *CD163*: a specific marker of macrophages in paraffin-embedded tissue samples. *Am J Clin Pathol*. 2004;122(5):794–801.
96. Gerbe F, Jay P. Intestinal tuft cells: epithelial sentinels linking luminal cues to the immune system. *Mucosal Immunol*. 2016;9(6):1353–9.
97. Rheinländer A, Schraven B, Bomhard U. *CD45* in human physiology and clinical medicine. *Immunol Lett*. 2018;196:22–32.
98. Zhu J, Yamane H, Cote-Sierra J, Guo L, Paul WE. *GATA-3* promotes Th2 responses through three different mechanisms: induction of Th2 cytokine production, selective growth of Th2 cells and inhibition of Th1 cell-specific factors. *Cell Res*. 2006;16(1):3–10.
99. Mise T, Iijima M, Inohaya K, Kudo A, Wada H. Function of *Pax1* and *Pax9* in the sclerotome of medaka fish. *Genesis*. 2008;46(4):185–92.
100. Douglas G, Cho MT, Telegrafi A, Winter S, Carmichael J, Zackai EH, et al. De novo missense variants in *MEIS2* recapitulate the microdeletion phenotype of cardiac and palate abnormalities, developmental delay, intellectual disability and dysmorphic features. *Am J Med Genet A*. 2018;176(9):1845–51.
101. Ushakumary MG, Riccetti M, Perl AK. Resident interstitial lung fibroblasts and their role in alveolar stem cell niche development, homeostasis, injury, and regeneration. *Stem Cells Transl Med*. 2021;10(7):1021–32.
102. Chou MY, Li HC. Genomic organization and characterization of the human type XXI collagen (*COL21A1*) gene. *Genomics*. 2002;79(3):395–401.
103. Vaughan EM, Miller AL, Hoi-Ying EY, Bement WM. Control of local Rho GTPase crosstalk by *Abr*. *Curr Biol*. 2011;21(4):270–7.
104. Bergström JH, Berg KA, Rodríguez-Piñeiro AM, Stecher B, Johansson ME, Hansson GC. *AGR2*, an endoplasmic reticulum protein, is secreted into the gastrointestinal mucus. *PLoS ONE*. 2014;9(8):e104186.
105. Umasuthan N, Xue X, Caballero-Solares A, Kumar S, Westcott JD, Chen Z, et al. Transcriptomic profiling in fins of Atlantic salmon parasitized with sea lice: evidence for an early imbalance between chalimus-induced immunomodulation and the host's defense response. *Int J Mol Sci*. 2020;21(7):2417.
106. Ullah R, Ansar M, Durrani ZU, Lee K, Santos-Cortez RL, Muhammad D, et al. Novel mutations in the genes *TGM1* and *ALOXE3* underlying autosomal recessive congenital ichthyosis. *Int J Dermatol*. 2016;55(5):524–30.
107. Zeissig S, Bürgel N, Günzel D, Richter J, Mankertz J, Wahnschaffe U, et al. Changes in expression and distribution of claudin 2, 5 and 8 lead to discontinuous tight junctions and barrier dysfunction in active Crohn's disease. *Gut*. 2007;56(1):61–72.
108. Houreld NN, Ayuk SM, Abraham H. Cell adhesion molecules are mediated by photobiomodulation at 660 nm in diabetic wounded fibroblast cells. *Cells*. 2018;7(4):30.
109. Bobowski-Gerard M, Boulet C, Zummo FP, Dubois-Chevalier J, Gheeraert C, Bou Saleh M, et al. Functional genomics uncovers the transcription factor *BNC2* as required for myofibroblastic activation in fibrosis. *Nat Commun*. 2022;13(1):5324.
110. Patterson LB, Parichy DM. Interactions with iridophores and the tissue environment required for patterning melanophores and xanthophores during zebrafish adult pigment stripe formation. *PLoS Genet*. 2013;9(5):e1003561.
111. Peretti T, Waisberg J, Mader AM, de Matos LL, da Costa RB, Conceição GM, et al. Heparanase-2, syndecan-1, and extracellular matrix remodeling in colorectal carcinoma. *Eur J Gastroenterol Hepatol*. 2008;20(8):756–65.
112. Puig-Kröger A, Corbi A. *RUNX3*: a new player in myeloid gene expression and immune response. *J Cell Biochem*. 2006;98(4):744–56.
113. Raverdeau M, Mills KH. Modulation of T cell and innate immune responses by retinoic acid. *J Immunol*. 2014;192(7):2953–8.
114. Han SB, Moratz C, Huang NN, Kelsall B, Cho H, Shi CS, et al. *Rgs1* and *Gnai2* regulate the entrance of B lymphocytes into lymph nodes and B cell motility within lymph node follicles. *Immunity*. 2005;22(3):343–54.
115. Maravillas-Montero JL, Santos-Argumedo L. The myosin family: unconventional roles of actin-dependent molecular motors in immune cells. *J Leukoc Biol*. 2012;91(1):35–46.
116. Kuwahara M, Yamashita M, Shinoda K, Tofukuji S, Onodera A, Shin-nakasu R, et al. The transcription factor *Sox4* is a downstream target of signaling by the cytokine *TGF-β* and suppresses TH2 differentiation. *Nat Immunol*. 2012;13(8):778–86.
117. Kumar A, Humphreys TD, Kremer KN, Bramati PS, Bradfield L, Edgar CE, Hedin KE. *CXCR4* physically associates with the T cell receptor to signal in T cells. *Immunity*. 2006;25(2):213–24.
118. Mathieson BJ, Sharrow SO, Bottomly K, Fowlkes BJ. *Ly9*, an alloantigenic marker of lymphocyte differentiation. *J Immunol*. 1980;125(5):2127–36.
119. Carow B, Rottenberg ME. *Socs3*, a major regulator of infection and inflammation. *Front Immunol*. 2014;5:58.
120. Martínez D, Oyarzún-Salazar R, Quilapi AM, Coronado J, Enriquez R, Vargas-Lagos C, et al. Live and inactivated *Piscirickettsia salmonis* activated nutritional immunity in Atlantic salmon (*Salmo salar*). *Front Immunol*. 2023;14:1187209.
121. Jennings ML. Cell physiology and molecular mechanism of anion transport by erythrocyte band 3/AE1. *Am J Physiol Cell Physiol*. 2021;321(6):C1028–59.
122. Huang SG, Zhang LL, Niu Q, Xiang GM, Liu LL, Jiang DN, et al. Hypoxia promotes epithelial-mesenchymal transition of hepatocellular carcinoma cells via inducing *GLIPR-2* expression. *PLoS ONE*. 2013;8(10):e77497.
123. Wee P, Wang Z. Epidermal growth factor receptor cell proliferation signaling pathways. *Cancers*. 2017;9(5):52.
124. Mou Y, Zhang L, Liu Z, Song X. Abundant expression of ferroptosis-related *SAT1* is related to unfavorable outcome and immune cell infiltration in low-grade glioma. *BMC Cancer*. 2022;22(1):1–15.
125. Chen J, Ingham N, Kelly J, Jadeja S, Goulding D, Pass J, et al. Spinster homolog 2 (*spns2*) deficiency causes early onset progressive hearing loss. *PLoS Genet*. 2014;10(10):e1004688.
126. Caldwell JM, Collins MH, Kemme KA, Sherrill JD, Wen T, Rochman M, et al. Cadherin 26 is an alpha integrin-binding epithelial receptor regulated during allergic inflammation. *Mucosal Immunol*. 2017;10(5):1190–201.
127. Wiche G. Commentary: role of plectin in cytoskeleton organization and dynamics. *J Cell Sci*. 1998;111(17):2477–86.
128. Granada L, Dirks RP, Ortiz-Delgado JB, Gavaia PJ, Sarasquete C, Laize V, et al. Warfarin-exposed zebrafish embryos resembles human warfarin embryopathy in a dose and developmental-time dependent manner—from molecular mechanisms to environmental concerns. *Ecotoxicol Environ Saf*. 2019;181:559–71.
129. Qian M, Chen Z, Wang S, Guo X, Zhang Z, Qiu W, et al. *PLEKHG5* is a novel prognostic biomarker in glioma patients. *Int J Clin Oncol*. 2019;24:1350–8.
130. Daggett DF, Boyd CA, Gautier P, Bryson-Richardson RJ, Thisse C, Thisse B, et al. Developmentally restricted actin-regulatory molecules control morphogenetic cell movements in the zebrafish gastrula. *Curr Biol*. 2004;14(18):1632–8.
131. Ma AC, Ward AC, Liang R, Leung AY. The role of *jak2a* in zebrafish hematopoiesis. *Blood*. 2007;110(6):1824–30.
132. Wu H, Huang M, Cao P, Wang T, Shu Y, Liu P. MiR-135a targets *JAK2* and inhibits gastric cancer cell proliferation. *Cancer Biol Ther*. 2012;13(5):281–8.
133. Sasaki A, Yasukawa H, Shouda T, Kitamura T, Dikic I, Yoshimura A. *CIS3/Socs-3* suppresses erythropoietin (*EPO*) signaling by binding the *EPO* receptor and *JAK2*. *J Biol Chem*. 2000;275(38):29338–47.
134. Podobnik M, Kisovec M, Anderluh G. Molecular mechanism of pore formation by aerolysin-like proteins. *Philos Trans R Soc B: Biol Sci*. 2017;372(1726):20160209.
135. Chen LL, Xie J, Cao DD, Jia N, Li YJ, Sun H, et al. The pore-forming protein Aep1 is an innate immune molecule that prevents zebrafish from bacterial infection. *Dev Comp Immunol*. 2018;82:49–54.
136. Xiong Y, Dan C, Ren F, Su Z, Zhang Y, Mei J. Proteomic profiling of yellow catfish (*Pelteobagrus fulvidraco*) skin mucus identifies differentially-expressed proteins in response to *Edwardsiella ictaluri* infection. *Fish Shellfish Immunol*. 2020;100:98–108.
137. Lee RT, Asharani PV, Carney TJ. Basal keratinocytes contribute to all strata of the adult zebrafish epidermis. *PLoS ONE*. 2014;9(1):e84858.

138. Leclerc-Mercier S, Lemoine R, Bigorgne AE, Sepulveda F, Leveau C, Fischer A, et al. Ichthyosis as the dermatological phenotype associated with *TTC7A* mutations. *Br J Dermatol*. 2016;175(5):1061–4.
139. Subramanian K, Neill DR, Malak HA, Spelmink L, Khandaker S, Marchiori GDL, et al. Pneumolysin binds to the mannose receptor C type 1 (*MRC-1*) leading to anti-inflammatory responses and enhanced pneumococcal survival. *Nat Microbiol*. 2019;4(1):62–70.
140. Robledo D, Gutiérrez AP, Barriá A, Yáñez JM, Houston RD. Gene expression response to sea lice in Atlantic salmon skin: RNA sequencing comparison between resistant and susceptible animals. *Front Genet*. 2018;9:287.
141. Palazón-Riquelme P, Worboys JD, Green J, Valera A, Martín-Sánchez F, Pellegrini C, Brough D, López-Castejón G. *USP7* and *USP47* deubiquitinases regulate *NLRP3* inflammasome activation. *EMBO Rep*. 2018;19(10):e44766.
142. Lecaudey LA, Schliwien UK, Osinow AG, Taylor EB, Bernatchez L, Weiss SJ. Inferring phylogenetic structure, hybridization and divergence times within Salmoninae (Teleostei: Salmonidae) using RAD-sequencing. *Mol Phylogenet Evol*. 2018;124:82–99.
143. Pike AW. Sea lice—major pathogens of farmed Atlantic salmon. *Parasitol Today*. 1989;5(9):291–7.
144. Fast MD, Burka JF, Johnson SC, Ross NW. Enzymes released from *Lepeophtheirus salmonis* in response to mucus from different salmonids. *J Parasitol*. 2003;89(1):7–13.
145. Fast MD, Muise DM, Easy RE, Ross NW, Johnson SC. The effects of *Lepeophtheirus salmonis* infections on the stress response and immunological status of Atlantic salmon (*Salmo salar*). *Fish Shellfish Immunol*. 2006;21(3):228–41.
146. Carr MM, McVittie E, Guy K, Gawkrödger DJ, Hunter JA. MHC class II antigen expression in normal human epidermis. *Immunology*. 1986;59(2):223.
147. Tamoutounour S, Han SJ, Deckers J, Constantinides MG, Hurabille C, Harrison OJ, et al. Keratinocyte-intrinsic MHCII expression controls microbiota-induced Th1 cell responses. *PNAS*. 2019;116(47):23643–52.
148. Holm HJ, Skugor S, Bjelland AK, Radunovic S, Wadsworth S, Koppang EO, Evensen Ø. Contrasting expression of immune genes in scaled and scaleless skin of Atlantic salmon infected with young stages of *Lepeophtheirus salmonis*. *Dev Comp Immunol*. 2017;67:153–65.
149. Barker JN, Griffiths CE, Nickoloff BJ, Mitra RS, Dixit VM. Keratinocytes as initiators of inflammation. *Lancet*. 1991;337(8735):211–4.
150. Cai W, Kumar S, Navaneethaiyer U, Caballero-Solares A, Carvalho LA, Whyte SK, et al. Transcriptome analysis of Atlantic salmon (*Salmo salar*) skin in response to sea lice and infectious salmon anemia virus co-infection under different experimental functional diets. *Front Immunol*. 2022;12. <https://doi.org/10.3389/fimmu.2021.787033>.
151. Robinson NA, Gjedrem T, Quillet E. Improvement of disease resistance by genetic methods. In: Jeney G. *Fish diseases*. Academic Press. 2017. p. 21–50.
152. Skugor S, Glover KA, Nilsen F, Krasnov A. Local and systemic gene expression responses of Atlantic salmon (*Salmo salar* L.) to infection with the salmon louse (*Lepeophtheirus salmonis*). *BMC Genomics*. 2008;9:1–18.
153. Swart M, Troeberg L. Effect of polarization and chronic inflammation on macrophage expression of heparan sulfate proteoglycans and biosynthesis enzymes. *J Histochem Cytochem*. 2019;67(1):9–27.
154. McManus CM, Maizels RM. Regulatory T cells in parasite infections: susceptibility, specificity and specialisation. *Trends Parasitol*. 2023;39(7):547–62.
155. Øvergård AC, Eichner C, Nuñez-Ortiz N, Kongshaug H, Borchel A, Dalvin S. Transcriptomic and targeted immune transcript analyses confirm localized skin immune responses in Atlantic salmon towards the salmon louse. *Fish Shellfish Immunol*. 2023;138:108835.
156. Wang L, Liu Y, Dai Y, Tang X, Yin T, Wang C, et al. Single-cell RNA-seq analysis reveals *BHLHE40*-driven pro-tumour neutrophils with hyper-activated glycolysis in pancreatic tumour microenvironment. *Gut*. 2023;72(5):958–71.
157. Fast MD, Johnson SC, Eddy TD, Pinto D, Ross NW. *Lepeophtheirus salmonis* secretory/excretory products and their effects on Atlantic salmon immune gene regulation. *Parasite Immunol*. 2007;29(4):179–89.
158. Braden LM, Monaghan SJ, Fast MD. Salmon immunological defence and interplay with the modulatory capabilities of its ectoparasite *Lepeophtheirus salmonis*. *Parasite Immunol*. 2020;42(8):e12731.
159. Núñez-Acuña G, Gonçalves AT, Valenzuela-Munoz V, Pino-Marambio J, Wadsworth S, Gallardo-Escárate C. Transcriptome immunomodulation of in-feed additives in Atlantic salmon *Salmo salar* infested with sea lice *Caligus rogercresseyi*. *Fish Shellfish Immunol*. 2015;47(1):450–60.
160. Wang T, Gorgoglione B, Maehr T, Holland JW, Vecino JL, Wadsworth S, Secombes CJ. Fish suppressors of cytokine signaling (SOCS): gene discovery, modulation of expression and function. *J Signal Transduct*. 2011;905813.
161. Zhang M, Xiao ZZ, Sun L. Suppressor of cytokine signaling 3 inhibits head kidney macrophage activation and cytokine expression in *Scophthalmus maximus*. *Dev Comp Immunol*. 2011;35(2):174–81.
162. Kittilsen S, Johansen IB, Braastad BO, Øverli Ø. Pigments, parasites and personality: towards a unifying role for steroid hormones? *PLoS ONE*. 2012;7(4):e34281.
163. Weinberg ED. Iron availability and infection. *Biochim Biophys Acta Gen Sub*. 2009;1790(7):600–5.
164. Ganz T, Nemeth E. Iron homeostasis in host defence and inflammation. *Nat Rev Immunol*. 2015;15(8):500–10.
165. Drakesmith H, Prentice A. Viral infection and iron metabolism. *Nat Rev Microbiol*. 2008;6(7):541–52.
166. Valenzuela-Muñoz V, Gallardo-Escárate C. Iron metabolism modulation in Atlantic salmon infested with the sea lice *Lepeophtheirus salmonis* and *Caligus rogercresseyi*: a matter of nutritional immunity? *Fish Shellfish Immunol*. 2017;60:97–102.
167. Fast MD, Ross NW, Craft CA, Locke SJ, MacKinnon SL, Johnson SC. *Lepeophtheirus salmonis*: characterization of prostaglandin E2 in secretory products of the salmon louse by RP-HPLC and mass spectrometry. *Exp Parasitol*. 2004;107(1–2):5–13.
168. Sutherland BJ, Koczka KW, Yasuie M, Jantzen SG, Yazawa R, Koop BF, et al. Comparative transcriptomics of Atlantic *Salmo salar*, chum *Oncorhynchus keta* and pink salmon *O. gorbuscha* during infections with salmon lice *Lepeophtheirus salmonis*. *BMC Genomics*. 2014;15:1–17.
169. Burka JF, Fast MD, Revie CW. *Lepeophtheirus salmonis* and *Caligus rogercresseyi*. In: Woo PTK, Buchmann K, editors. *Fish parasites: pathobiology and protection*. Wallingford UK: Cabi; 2012. p. 350–70.
170. Sheldon JR, Skaar EP. Metals as phagocyte antimicrobial effectors. *Curr Opin Immunol*. 2019;60:1–9.
171. Caballero-Solares A, Umasuthan N, Xue X, Katan T, Kumar S, Westcott JD, et al. Interacting effects of sea louse (*Lepeophtheirus salmonis*) infection and formalin-killed *Aeromonas salmonicida* on Atlantic salmon skin transcriptome. *Front Immunol*. 2022;13. <https://doi.org/10.3389/fimmu.2022.804987>.
172. Ruiz Daniels R, Taylor RS, Robledo D, Macqueen DJ. Single cell genomics as a transformative approach for aquaculture research and innovation. *Rev Aquac*. 2023;15(4):1618–37.
173. Robinson NA, Østbye TKK, Kettunen AH, Coates A, Barrett LT, Robledo D, Dempster T. A guide to assess the use of gene editing in aquaculture. *Rev Aquac*. 2024;16(2):775–84.
174. Ruiz Daniels R, Taylor RS, Dobie R, Salisbury S, Furniss JJ, Clark E, et al. A versatile nuclei extraction protocol for single nucleus sequencing in non-model species—optimization in various Atlantic salmon tissues. *PLoS ONE*. 2023;18(9):e0285020.
175. Dobin A. STAR manual 2.7. 0a. Weill Cornell Medicine. 2019.
176. Kaminow B, Yunusov D, Dobin A. STARsolo: accurate, fast and versatile mapping/quantification of single-cell and single-nucleus RNA-seq data. *BioRxiv*. 2021. <https://doi.org/10.1101/2021.05.05.442755>.
177. Perteau G, Perteau M. GFF utilities: GffRead and GffCompare. *F1000Research*. 2020;9:ISCB Comm J-304.
178. R Core Team. R: a language and environment for statistical computing. R Foundation for Statistical Computing, Vienna, Austria. 2021; URL <https://www.R-project.org/>.
179. Hao Y, Hao S, Andersen-Nissen E, Mauck WM, Zheng S, Butler A, et al. Integrated analysis of multimodal single-cell data. *Cell*. 2021;184(13):3573–87.
180. Ahlmann-Eltze C, Huber W. glmGamPoi: fitting Gamma-Poisson generalized linear models on single cell count data. *Bioinformatics*. 2020;36(24):5701–2.
181. McGinnis CS, Murrow LM, Gartner ZJ. DoubletFinder: doublet detection in single-cell RNA sequencing data using artificial nearest neighbors. *Cell Syst*. 2019;8(4):329–37.

182. Maglott D, Ostell J, Pruitt KD, Tatusova T. Entrez Gene: gene-centered information at NCBI. *Nucleic Acids Res.* 2005;33(suppl_1):D54–8.
183. UniProt Consortium. UniProt: a worldwide hub of protein knowledge. *Nucleic Acids Res.* 2019;47(D1):D506–15.
184. Smedley D, Haider S, Ballester B, Holland R, London D, Thorisson G, Kasprzyk A. BioMart—biological queries made easy. *BMC Genomics.* 2009;10(1):1–12.
185. Ge SX, Jung D, Yao R. ShinyGO: a graphical gene-set enrichment tool for animals and plants. *Bioinformatics.* 2020;36(8):2628–9.
186. Emms DM, Kelly S. OrthoFinder: phylogenetic orthology inference for comparative genomics. *Genome Biol.* 2019;20:1–14.
187. Salisbury SJ, Ruiz Daniels R, Monaghan SJ, Bron JE, Villamayor PR, Gervais O, et al. 2024. GEO <https://www.ncbi.nlm.nih.gov/geo/query/acc.cgi?acc=GSE269132>.

Publisher's Note

Springer Nature remains neutral with regard to jurisdictional claims in published maps and institutional affiliations.